APPLYING ADVANCED SPATIAL ANALYSIS METHODS TO DEVELOP A SCIENTIFICALLY ROBUST ANTICIPATORY FRAMEWORK FOR FORECASTING DESERTIFICATION PATTERNS IN JAHUN, JIGAWA STATE, NIGERIA

IBRAHIM, I. Y.[1,2] – WANG, Y. D.[1*] – UMAR, D. D.[3] – IBRAHIM, B. M.[4] – OGBUE, C. P.[1,2] – ABUBAKAR, Y. I.[5] – HAMISU, A. B.[6] – MUHAMMAD, B. D.[7]

[1]*National Engineering Technology Research Center for Desert-Oasis Ecological Construction, Xinjiang Institute of Ecology and Geography Chinese Academy of Sciences, Urumqi 830011, China*

[2]*University of Chinese Academy of Sciences, Beijing 100049, China*

[3]*Department of Agronomy, Bayero University, Kano 700001, Nigeria*

[4]*Africa Desertification Control Initiative, Kano 700001, Nigeria*

[5]*Federal Polytechnic, Daura, Katsina State 820001, Nigeria*

[6]*Department of Urban and Regional Planning, Hussain Adamu Federal Polytechnic, Kazaure, Jigawa State 705101, Nigeria*

[7]*MB Dan' Azumi & Co (Legal Practitioners, Chartered Mediators, Notaries Public), Kano 700001, Nigeria*

**Corresponding author*
e-mail: wangyd@ms.xjb.ac.cn

(Received 4th Feb 2024; accepted 3rd May 2024)

Abstract. Desertification, a formidable environmental challenge with broad implications for ecosystems and communities, is examined within Jahun Local Government Area in Jigawa State, Nigeria. This study uses a Cellular Automata Markov Chain Analysis model to visualize and predict the associated environmental risks. Objectives include assessing the extent and rate of desertification in the region and forecasting the process until 2080. Utilizing a multidisciplinary approach, the research integrates unsupervised classification of Landsat images, Land Use Land Cover (LUCC) analysis using MODIS data, Maximum Likelihood classification, and cubic trend analysis. The outcomes yield a comprehensive understanding of desertification dynamics in Jahun Local Government Area, identifying susceptible areas for environmental degradation. The study revealed significant changes in various land cover types within the research area. Urban areas experienced a substantial annual increase of 6.3030 km^2, suggesting dynamic transformations within urban landscapes, possibly driven by shifts in population density, infrastructure development, or land use patterns. Conversely, vegetation exhibited a higher rate of change, with an annual decrease of 9.3787 km^2, indicating variations in vegetative cover. Waterbodies displayed minimal changes, with a slight reduction rate of 0.2723 km^2/year. In contrast, bare lands demonstrated a notable increase, expanding at a rate of 15.9541 km^2/year, underscoring significant alterations in these regions. The observed variations in rates of change emphasize the dynamic nature of land cover in the study region and underscore the importance of understanding these changes for effective environmental management and policymaking. The study's predictions up to 2080 offers crucial insights for stakeholders and policymakers, facilitating the formulation of proactive monitoring and management strategies to effectively combat desertification and mitigate its adverse effects on ecosystems and livelihoods.

Keywords: *desertification, cellular automata, Markov chain analysis, predictive modelling, desertification trends, land cover change*

http://www.aloki.hu ● ISSN 1589 1623 (Print) ● ISSN 1785 0037 (Online)
DOI: http://dx.doi.org/10.15666/aeer/2204_36413676

Introduction

The United Nation (UN) 2030 agenda, with its focus on sustainable development, addresses critical issues aimed at creating a world where fundamental rights are safeguarded, and inequality is diminished. While the connection between the UN 2030 agenda and desertification may not be immediately apparent, it is important to recognize that sustainable development encompasses a broad spectrum of interrelated goals, including environmental protection, social equity, and economic prosperity. Desertification, as a significant environmental challenge, directly impacts the well-being of communities, exacerbates inequalities, and threatens fundamental rights such as access to food, water, and livelihoods. Therefore, efforts to combat desertification align with the overarching objectives of the UN 2030 agenda by promoting environmental sustainability, social inclusivity, and economic resilience (UN, 2015). Scientists from various fields are concerned about inappropriate soil management practices because of their tight relationship to food security and climate change (Gomiero, 2016). Soil conservation, however, remains a minor concern for numerous government bodies and does not spark passionate debate. Furthermore, reaching key objectives for global reforms will be extremely difficult. As a result, worldwide sensitive areas to desertification are still rising, which can lead to major issues in supporting life on the planet (da Silva et al., 2023). Desertification, a complex and dynamic system of land deterioration prevalent in drylands, is defined in the main text of the United Nations Conference on Environment and Development (Kassas, 1995; UNCCD, 1992) as land degradation in arid, semi-arid, and dry sub-humid areas caused by various factors such as climatic variations and human activities (Zongfan et al., 2022). This phenomenon, which signifies the depletion of dry, semi-arid, and sub-humid habitats, is a critical concern that needs to be addressed. To develop effective strategies for land rehabilitation and combating global desertification in vulnerable areas, it is essential to assess the susceptibility of global-scale desertification to climate change and human activities. However, as noted by (Huang et al., 2020). no global map currently considers climate change and human activity in evaluating vulnerability to desertification.

Desertification in drylands, as detailed by Abuzaid and Abdelatif (2022), is a complex process of land deterioration resulting from the interaction of various physical, biological, political, social, economic, and cultural factors along with climatic changes in arid, semi-arid, and dry sub-humid areas. This definition aligns with the broader understanding provided by Pravalie (2021) and Pravalie et al. (2021), who describe desertification as land degradation in specific climatic zones, and further echoed by Lamchin et al. (2016), highlighting the role of weather fluctuations and human activity. As expounded by Huber-Sannwald et al. (2020) it aggravates droughts, food shortages, poverty, violence, emigration, political instability, and societal disintegration. The United Nations Convention to Combat Desertification (UNCCD, 2010) views it as an extreme form of land degradation characterized by a significant decline in land's biological and economic productivity. The relationship between desertification and poverty is especially noteworthy. Studies by Wang (2003) and do Nascimento (2023) underscore poverty as both a consequence and a catalyst of desertification. Olsson (1993) emphasizes that rural poverty, often exacerbated by biased pricing and dysfunctional markets, drives communities towards unsustainable land use, perpetuating the cycle of land degradation and poverty. Since its introduction in the United Nations Conference on Desertification in 1977, the term 'desertification' has been central to

http://www.aloki.hu ● ISSN 1589 1623 (Print) ● ISSN 1785 0037 (Online)
DOI: http://dx.doi.org/10.15666/aeer/2204_36413676

development debates, often mistakenly blamed for various socio-economic issues in Africa due to its complex and multifaceted nature. Global desertification hotspots represented a 9.2% reduction in land productivity, affecting about 500 million people in, 2015, impacting agricultural production, mainly in regions of Asia, Africa, and the Middle East (Masson-Delmotte, 2019). According to UNEP's 1984 findings, the challenge of desertification is intensifying, with the Sahara Desert encroaching on arable and pasture lands at an alarming rate of 1.5 million hectares annually. This expanding desertification poses a significant threat to approximately 35% of the African continent, notably affecting regions like Mediterranean Africa, the Sudano-Sahelian area, and the areas south of the Sudano-Sahelian region. Over the past half-century, Africa has witnessed the loss of around 650,000 km^2 of fertile agricultural land, a concerning trend highlighted in recent research by Ibrahim et al. (2023). The human impact of this environmental crisis is profound. As reported by Darkoh (1989), at least 36% of Africa's population in 1983 – equating to about 185.5 million out of the total 513 million people were directly affected by desertification. This situation presents a severe ecological challenge and has far-reaching implications for food security, livelihoods, and the overall socio-economic stability of the affected regions.

The Sahel region of Africa is facing a severe environmental crisis, highlighted by various initiatives and research efforts to combat desertification and land degradation. A notable initiative is the Great Green Wall of Africa, proposed by Sahel countries with the ambitious goal of eradicating soil degradation by 2030, as noted by Yang et al. (2022). Supporting this initiative, research by Berrahmouni et al. (2016) indicates that the recoverable degraded land in the Sahel amounts to approximately 166 million hectares, requiring a yearly restoration rate of over 10 million hectares. However, challenges to reforestation efforts are significant, as reported by Benjaminsen and Hiernaux (2019), who note that more than 80% of the reforested trees have died thus far. Adding to these challenges, Policelli et al. (2019) highlight the drastic decline of Lake Chad's area by over 90%, due to natural factors like drought and human-induced factors including population growth, farmland reclamation, and large-scale irrigation. Further, (Tierney et al., 2015) observed clear drought trends in the Horn of Africa from 1901 to 2010, exacerbating the desertification issue in the Sahel. On a positive note (Yang et al., 2022) discovered that the climate in the Sahel has become more humid in the last 30 years, with an increase in vegetation and canopy coverage. Corroborating this, Giannini et al. (2013), Brandt et al. (2020), and Yang et al. (2022) found evidence of re-greening in the region, especially along the Mali-Niger border. Yet, the environmental situation remains precarious due to practices like cattle raising, bush clearing for agriculture, and deforestation, which have severely degraded the environment, as noted by Sop and Oldeland) (2013). In Nigeria, one of the most affected countries, the main causes of desertification are human activities and adverse climatic conditions. Cotthem (2007) explains that population demands exert stress on the ecosystem, impacting various aspects such as livestock, crop output, and the supply of fuel wood and building materials. Audu (2013) points out that the demand for fuel wood is particularly high in rural areas due to its availability, affordability, and traditional usage, compounded by the lack of alternative indigenous fuel sources. Nigeria, as reported by (Food and Agriculture Organization (FAO) of the United Nations, 2005) has the highest rate of primary forest deforestation worldwide and is most visibly affected by desertification in its Sudano-Sahel dry land region, encompassing states like Sokoto, Katsina, Kebbi, Kano, Jigawa, Zamfara, Yobe, and

http://www.aloki.hu ● ISSN 1589 1623 (Print) ● ISSN 1785 0037 (Online)
DOI: http://dx.doi.org/10.15666/aeer/2204_36413676

Borno. Tomasella et al. (2018) emphasizes the importance of continuous monitoring of land use and land cover changes in drylands, which are typically prone to rapid soil erosion, land degradation, and desertification, resulting in significant losses of vegetation cover. This knowledge is crucial for the effective management of drylands and supporting sustainable soil use decisions.

In Jahun, located in Jigawa State, Nigeria, a region deeply affected by the environmental crisis of desertification, our study proposes a critical and innovative approach. This area, known for its Sahel and Sudano-Sahelian climate, is facing severe soil degradation, water scarcity, and agricultural difficulties (*Fig. A1* in the *Appendix*). Building upon the work of Reynolds et al. (2007), who offer a comprehensive understanding of global desertification drivers, our research incorporates the advanced predictive methodologies emphasized by Huang et al. (2020). These methodologies are crucial for accurately forecasting desertification patterns, especially in regions like Jahun. Additionally, the socio-economic impacts of desertification, particularly relevant to Jahun, are explored in line with the insights provided by Shuai et al. (2021). Three key aspects of our study area are highlighted. Firstly, the unique climatic and geographical conditions of Jahun that exacerbate land degradation; secondly, the socio-economic fabric of the region, characterized by agricultural dependency and vulnerability to climatic variations; and thirdly, the lack of prior comprehensive studies focusing on this specific region, making our research not only novel but also critical for regional environmental planning and management. Our study, therefore, stands as a significant contribution to the understanding of desertification processes, providing a model that can be adapted for similar regions globally, and offering valuable insights for environmental policy and sustainable land management. The advent of remote sensing technologies has revolutionized the way researchers monitor desert expansion, as highlighted by Yang et al. (2022) and Zeng et al. (2006).

This technological advancement has been instrumental in enhancing desertification modeling, a critical process for predicting and visualizing the potential environmental impacts of desertification, as underscored in studies by Falaki et al. (2020) and Yunusa (2012). Despite the development of several simulation models designed to forecast and map desertification, their application remains limited to a small fraction of the vast global areas affected by this phenomenon. These models are invaluable for predicting the occurrence of desertification in areas most susceptible to this issue. To address this, our study employed a cellular automata Markov chain analysis model, focusing on the Jahun Local Government area in Jigawa State, Nigeria. This approach is aimed at visualizing and predicting the expected environmental risk towards desertification in the region. The study's objectives are twofold: firstly, to quantify the extent and rate of desertification within the study area, and secondly, to project the progression of desertification up to the year 2080. By doing so, this research seeks to provide reliable monitoring and management strategies to mitigate desertification in the targeted area, offering a vital resource for environmental planning and policy formulation.

Materials and methods

The study area

One of Jigawa State's twenty-seven local government areas, Jahun Local Government, was established in 1976 and is located between latitudes 12°04′0″N and 9°38′0″E (*Fig. 1*). It is divided into four districts: Jahun, Aujara, Gunka and

http://www.aloki.hu ● ISSN 1589 1623 (Print) ● ISSN 1785 0037 (Online)
DOI: http://dx.doi.org/10.15666/aeer/2204_36413676

Kadawawa. It shares boundaries with the local governments of Taura and Kaugama in the north, Kafin Hausa and Miga in the west, Kiyawa in the south, and Dutse and Ringim in the west. Jahun serves as the administrative center for the Jahun local government area, which is situated in Jigawa State in Nigeria's north-western geopolitical zone. Numerous towns and villages, including Aujara, Gunka, Damutawa, Tukunyawa, Gangawa, Chanmbe, Idanduna, and Doro, are included in the LGA. According to the 2006 census, Jahun LGA had an estimated 229,094 residents, Jahun LGA has a total size of 1172 km^2 with an average temperature of 33°C. The average wind speed in the area is 11 km/h, and total precipitation in the LGA is predicted to be 900 mm yearly (Abdullahi et al., 2023). Farming is an essential economic activity in Jahun LGA, where crops like onions, millet, and sweet potatoes are cultivated. Animal rearing, such as camels, rams, cows, and sheep, is also a thriving sector in Jahun LGA. Hunting, ceramics, and trading are other key economic pursuits for the residents of Jahun LGA.

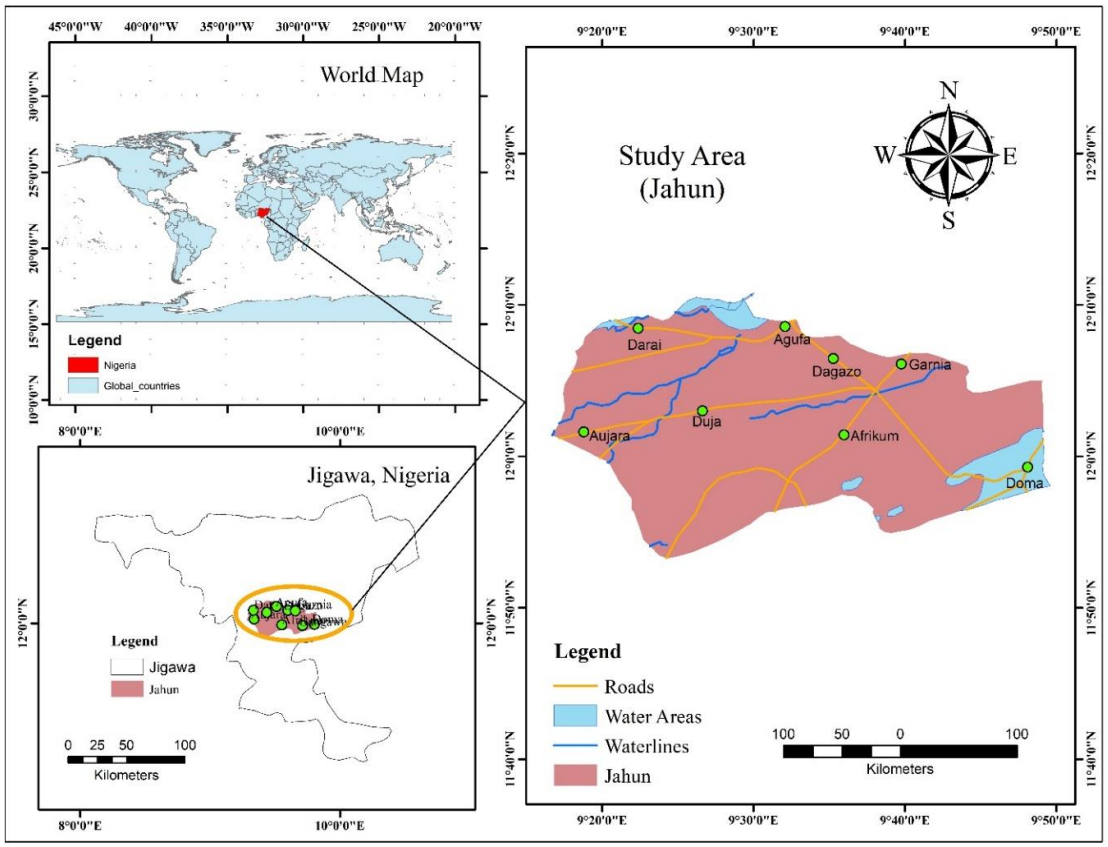

Figure 1. *Jahun Jigawa, Nigeria*

Desertification is not solely determined by precipitation levels but is influenced by a myriad of factors including land use practices, soil degradation, and vegetation cover. Despite the apparent abundance of rainfall, desertification processes can still occur due to unsustainable land management practices and other environmental stressors (D'Odorico et al., 2013).

Studies and observations from various regions around the world have shown that desertification can manifest even in areas with relatively high precipitation levels

http://www.aloki.hu ● ISSN 1589 1623 (Print) ● ISSN 1785 0037 (Online)
DOI: http://dx.doi.org/10.15666/aeer/2204_36413676

(D'Odorico et al., 2013). For instance, as per Williams et al. (2015) the global distribution of mean annual precipitation over the period 1901–2009 indicates that regions with low precipitation tend to be situated in specific geographical conditions: Low precipitation areas are often found inland, away from seas and oceans, which are primary moisture sources. The Gobi Desert in China is an example of such continental influence. Additionally, regions located on the leeward side of mountain ranges typically receive less precipitation due to the rain shadow effect. For instance, the Mojave Desert in North America experiences reduced rainfall as a result. Tropical areas, where air mass divergence is common due to the Hadley and Farrell circulations, also tend to have low precipitation. This includes the Sahara and Arabian deserts, as well as drylands in Australia and Patagonia. Moreover, proximity to cold ocean surfaces can lead to persistent air subsidence, resulting in low precipitation levels. Examples include the Namib desert in Southern Africa and the Atacama Desert in South America. Addressing desertification remains paramount regardless of the prevailing precipitation levels. The consequences of desertification, including soil erosion, loss of biodiversity, and impacts on local communities, necessitate urgent action. Therefore, it is imperative to implement appropriate mitigation and adaptation measures to combat desertification and safeguard the region's ecosystems and livelihoods.

Data acquisition

For this study, freely accessible datasets were obtained from governmental and/or scientific websites, including the United State Geological Survey (USGS https://www.usgs.gov/), Earth Engine Data Catalog (https://developers.google.com/earthengine/datasets/catalog/landsat). A more detailed description and application of the datasets is presented in the following sections. In this study, we used satellite images, and various secondary sources, including both published and unpublished articles, theses, projects, and other relevant documents. We employed specialized software tools such as Environmental Visualizing Imaging (ENVI), IDRISI Terrset, and Earth Resources Data Analysis System (ERDAS) for our analysis. To validate the reliability and consistency of our image classification process, we used Kappa statistics, a measure of agreement beyond chance. The Kappa values for the years 2000, 2010, and 2020 were 0.8683, 0.9233, and 0.9143, respectively, showing a high level of classification accuracy These values suggest that our classification process was robust over time (*Table 1*).

Table 1. *The accuracy statistics of supervised classification*

Year	Classification accuracy (%)	Kappa
2000	91.16	0.8683
2010	94.44	0.9233
2020	93.84	0.9143

Table 1 provides the accuracy statistics of our supervised classification, including the classification accuracy percentages and Kappa values for the years 2000, 2010, and 2020. Utilizing bands b3, b4, and b5 from Landsat 5, and bands b2, b3, and b4 from Landsat 8, we examined the scope and advancement of desertification within the study area using processed images in both ENVI and ERDAS Imagine. Feature classes were

http://www.aloki.hu ● ISSN 1589 1623 (Print) ● ISSN 1785 0037 (Online)
DOI: http://dx.doi.org/10.15666/aeer/2204_36413676

identified through visual interpretation, as outlined in *Table 2*. Over a 20-year span, from 2000 to 2020, we estimated the extent of desertification and compared the area coverage statistics derived from the classified images for these years to assess changes. To calculate the percentage change in desertification, we used the formula:

$$\text{Percentage change} = \left(\frac{x}{y}\right) x\ 100 \qquad \text{(Eq. 1)}$$

where x is the Observed Change: This refers to the difference in the extent of desertification between two time periods (e.g., 2000 and 2020). We quantified this by comparing the area covered by desertified land in each year using the feature classes identified through visual interpretation. y is the Sum of Changes: This represents the total change in desertification over the entire 20-year period under consideration. We calculated this by summing up the observed changes for each year within the specified timeframe.

Table 2. *Land use/land cover classification scheme*

Classes	Description
Urban	Frequently denotes populated or urban areas. Residential, commercial, and industrial zones can be included in this. Manufactured buildings, roads, and infrastructure define urban regions
Vegetation	Shades of green could symbolize vegetation, such as woods, meadows, and croplands
Waterbodies	It usually depicts large, open bodies of water, such as lakes, reservoirs, and deep rivers. These water features have a lot of water covering and are more extensive and profound
Bare lands	reflects regions used for agriculture or crops in a land use and land cover analysis. This group comprises regions where different crops are grown for agricultural purposes, cultivated fields, and farmland (Falaki et al., 2020)
Shallow water	Represents shallow bodies of water, including ponds, marshes, and coastal areas with relatively shallow depths
Specialized urban	Denotes specific urban areas with unique characteristics or functions, such as industrial parks, residential complexes, or historic districts

By applying *Equation 1*, which relates the observed change to the sum of changes, we were able to compute the percentage change in desertification over the 20-year period (Falaki et al., 2020). To project future desertification patterns up to 2080, we used a Cellular Automata Markov Chain analysis integrated within the IDRISI Terrset software. This method allowed us to model and predict the likely progression of desertification in the study area.

Tables 3 and *4* present the remote sensing image data used in this study, including sensor details, path/row, date, resolution, and cloud cover for the years 2000, 2010, and 2020.

http://www.aloki.hu ● ISSN 1589 1623 (Print) ● ISSN 1785 0037 (Online)
DOI: http://dx.doi.org/10.15666/aeer/2204_36413676

Table 3. *The data of remote sensing images used in this study*

Year	2000	2010	2020
Sensor	Landsat TM5	Landsat TM5	Landsat Oli
Path/row	188/052	188/052	188/052
Date	5/April/2000	1/April2010	10/April/2020
Resolution	30 m	30 × 30	30 × 30
Cloud Cover	5.00	11.00	13.00

Table 4*. Satellite imagery used in the study*

Satellite datasets	Spatial/temporal resolution	Time coverage	Data source
Landsat 7(ETM+)	98.2-degree\16-days	2000	https://earthexplorer.usgs.gov/
Landsat 7(ETM+)	98.2-degree\16-days	2010	https://earthexplorer.usgs.gov/
Landsat 8 (OLI)	98.2◦degree/705 km/16 days	2020	https://earthexplorer.usgs.gov/
MODIS	0.05◦ × 0.05◦\1-2 days	2000	https://earthengine.google.com/
MODIS	0.05◦ × 0.05◦\1-2 days	2010	https://earthengine.google.com/
MODIS	0.05◦ × 0.05◦ /1-2 days	2020	https://earthengine.google.com/

Source: Authors' analysis (2023)

Unsupervised classification

Unsupervised classification in remote sensing is a technique used to automatically group pixels in an image based on their spectral properties. This method is crucial for identifying patterns or natural groupings in the data without prior labeling. As outlined by Bernabé and Plaza (2010), this process involves clustering pixels so that those within the same group exhibit similar spectral characteristics. In our study, we utilized two renowned methods for unsupervised clustering: ISODATA and k-means. The ISODATA algorithm is a squared-error clustering technique. It starts with randomly assigning the image's pixel vectors into several initial clusters and then iteratively refines these clusters. Each iteration recalculates the partition of the image into clusters (Pi) with the goal of minimizing the squared error. This error, for a given partition Pi of the hyperspectral image into c clusters, is calculated as follows:

$$e^2(pi) = \sum_{k=1}^{c} \sum_{j=1}^{mik} (xjk - ck)^2 \qquad \text{(Eq. 2)}$$

where Ck– denotes the centroid of the k-th cluster; xjk– represents the pixels in the k-th cluster on iteration i, with mik– being the number of pixels in that cluster.

The algorithm continues to adjust the clusters to reduce the squared error in each iteration, based on *Equation 2*, until a convergence criterion is met. One challenge with ISODATA is setting the appropriate number of clusters (c) in advance.

For land use and land cover classification in the study area, we categorized the land into several classes These include urban areas, vegetation, waterbodies, bare lands, shallow water, and specialized urban, each with distinct characteristics identifiable through their spectral signatures.

http://www.aloki.hu ● ISSN 1589 1623 (Print) ● ISSN 1785 0037 (Online)
DOI: http://dx.doi.org/10.15666/aeer/2204_36413676

Supervised classification

Maximum likelihood classification

The maximum likelihood classification (MLC) technique is based on statistical principles, particularly the probability discriminant function and Bayesian discriminant rule. This method, as Li et al. (2020) explain, assumes that the statistical distribution of each pixel value for each image band follows a normal distribution. To perform this classification, we first define a 'region of interest' for each category we want to identify. Then, we calculate the mean and variance for these regions. Each pixel in the image is then classified based on which category's statistical profile it matches most closely, essentially determining the category with the highest likelihood for each pixel. The formula for the classification algorithm is as follows:

$$gk(xi) = \text{Ln}\, p(wk) - \frac{1}{2}\sum\nolimits_{k}^{-1} - \frac{1}{2}(xi - mi)^{T}\sum\nolimits_{k}^{-1}(xi - mi) \qquad \text{(Eq. 3)}$$

where gk(xi) – is the weighted distance, p(wk) – is the probability of the class belonging to category k, Σk – is the covariance matrix, and xi, mi – are the pixel's measurement vector and the sample mean of the i-th class, respectively.

For our study, we utilized visible, infrared, and near-infrared bands to measure the pixel's measurement vector for Land Use Land Cover (LUCC) classification. These bands were stacked and mosaicked together using Erdas Imagine 2016 software. Several satellite images were categorized using supervised classification with the MLC method, as practiced in studies by Baqa et al. (2022) and Tariq et al. (2022). Accuracy evaluation is crucial to determine how effectively the pixels were grouped into the correct land cover categories. For this purpose, we used Landsat high-resolution images, Google Earth, and Google Maps as reference points. The overall Kappa statistic and related classification accuracy measures were obtained using the formulation provided by Rwanga and Ndambuki (2017). Kappa analysis, a discrete multivariate method described by Jensen (1996), was used for accuracy evaluations. The Khat statistic, as defined by Congalton (1991) estimates the Kappa value and measures the agreement or correctness of the classification. It is calculated as follows:

$$k = \frac{x_{ii} - \sum_{i=1}^{r}(xi + xt1)}{N^{2} - \sum_{i=1}^{r}(xii + x + 1)} \qquad \text{(Eq. 4)}$$

LUCC transition analysis

For analyzing the transitions in Land Use Land Cover (LUCC) over time, we employed the Land Change Modeler (LCM) within the Terrset software (formerly known as IDRISI). The LCM is an advanced tool specifically designed for studying how land cover changes over time. It follows a step-by-step approach that involves several key processes:

1. Change Analysis: This initial step involves examining the differences in land cover between different times. By comparing Landsat imagery from different years, we can see how land use has changed.
2. Transition Potential Computing: In this phase, the model computes the likelihood of different types of land cover transitioning from one state to another. This helps us understand the factors driving these changes.

http://www.aloki.hu ● ISSN 1589 1623 (Print) ● ISSN 1785 0037 (Online)
DOI: http://dx.doi.org/10.15666/aeer/2204_36413676

3. Change Prediction: Finally, the model predicts future changes in land cover based on the observed patterns and computed transition potentials.

In conjunction with the LCM, we also used the Cellular Automata-Markov Chain model (CA-Markov). This model helps in understanding the probabilities of different land cover transitions, offering a more dynamic and probabilistic view of how land cover might change in the future. To ensure the accuracy of our analysis, we first assessed the accuracy of the Landsat imagery using Terrset 2020. Once the imagery was validated, we applied the cross-tabulation method. This method allows us to calculate the net changes in each LUCC category in square kilometers. We also examined the patterns of area exchanges, as well as the gains and losses for each LUCC class. These analyses were conducted for two distinct periods: from 2000 to 2010, and from 2010 to 2020. This approach provides a comprehensive view of how land use and land cover have evolved over these two decades and allows us to make more informed predictions about future changes. More information on LCM can be found on Clark lab (https://clarklabs.org/terrset/land-change-modeler/).

CA-Markov chain model

The integration of Cellular Automata (CA) with the Markov Chain model has become increasingly important in predicting urban expansion and land use changes. This method has been effectively used in various studies (Mansour et al., 2022; Mumtaz et al., 2020; Tariq et al., 2022; Wang et al.,2013). The Markov Chain model is particularly useful for forecasting future land use changes by analyzing the transition of Land Use Land Cover (LUCC) states over two time periods. It calculates the rate at which different land use types are likely to change into other types, providing a quantitative basis for predictions (Fan et al., 2008). A key assumption of the Markov model is that the current state of each spatial location (or pixel) can be used to predict future changes, including the influence of neighboring pixels (Tariq et al., 2022). This is where the Cellular Automata model complements the Markov Chain model. While the CA model focuses on identifying spatial changes, the Markov Chain model extends this by forecasting future spatiotemporal changes (Ahmed and Ahmed, 2012). The mathematical formulation of the CA-Markov model is as follows:

$$S(t+1) = ij * S(t) \qquad \text{(Eq. 5)}$$

where S(t) – is the land use status at time; t, S(t + 1) – is the land use status at time t, S, (t + 1); and Pij – is the transition probability matrix.

The transition probability matrix Pij is a key component of the model, indicating the likelihood of each land use type transitioning to another type. This matrix is defined as:

$$pij = \begin{Bmatrix} P_{1,1} & P_{2,1} & P_{N,1} \\ P_{1,2} & P_{2,2} & P_{N,2} \\ P_{1,N} & P_{2,N} & P_{N,N} \end{Bmatrix} \qquad \text{(Eq. 6)}$$

with each element pij ranging from 0 to 1 (Singh et al., 2018). This matrix is fundamental in determining the likely transitions between different land use states over time, thus enabling accurate predictions of future land use changes. The methodology

http://www.aloki.hu ● ISSN 1589 1623 (Print) ● ISSN 1785 0037 (Online)
DOI: http://dx.doi.org/10.15666/aeer/2204_36413676

flow diagram for the investigation is depicted in *Figure 2*. For a better understanding, see the detailed process flowchart below.

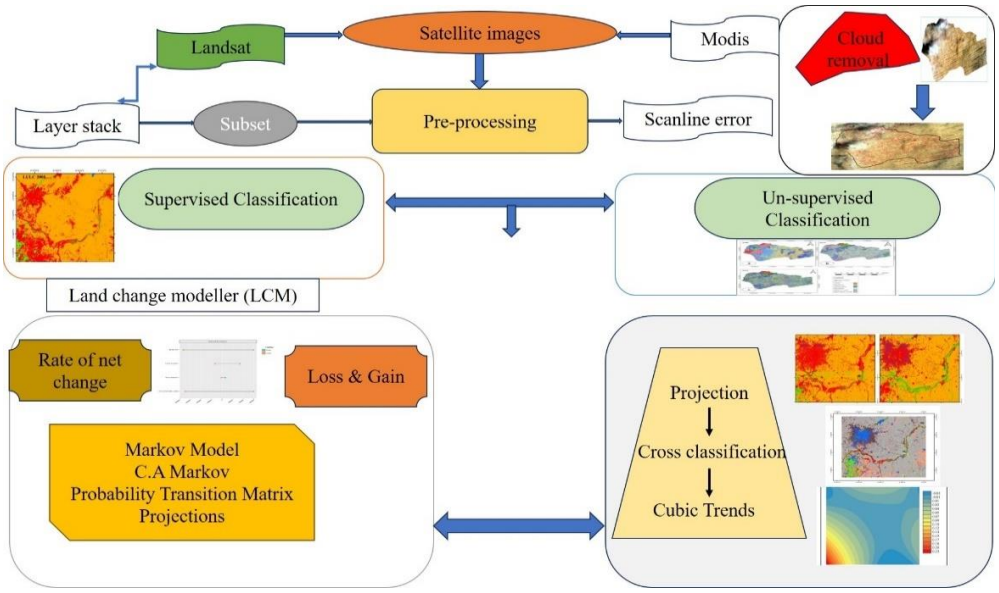

Figure 2. *Methodology's workflow chat*

Use of CA-Markov analysis to predict desertification in Jahun

IDRISI Selva 17.0, developed by Clark Labs in the United States of America, is a comprehensive image processing and Geographical Information System (GIS) program with over 300 modules designed for advanced geographical information analysis and visualization (Tariq, 2020). This platform includes a wide range of tools for environmental control, policy support, risk identification, simulation, and surface characterization. The Markov Chain model, as described by Aaviksoo (1995) and Araya and Cabral (2010), is an effective method for analyzing land use changes over time. It computes a sequence of values based on the current state, making it particularly suitable for forecasting temporal changes in land use (Mushore, et al., 2016; Dimitrios Triantakonstantis, 2012). Its capability to predict complex system dynamics makes it an invaluable tool in our analysis (Tariq, 2020). Cellular Automata (CA), chosen for its simplicity and effectiveness, is utilized to map spatial distribution and anticipate desertification sensitivity (Falaki et al., 2020). CA is particularly adept at modeling urban expansion and its effects on Land Surface Temperature (LST), as demonstrated in studies by Araya and Cabral (2010) and Garcia-Frapolli et al. (2007).

In our study, we employed the combined Cellular-Automata and Markov-Chain (CA-Markov chain) models within Terrset 2020 to analyze LUCC distributions from 2000 to 2020 and project future land cover from 2000 to 2080 and 2020 to 2080 (Falaki et al., 2020; Tariq, 2020). The Markov Chain analysis produced change probability maps, which served as inputs to the CA model. This integration allowed us to map future LUCC distributions and revealed spatiotemporal shifts in land use and land cover. We evaluated their effectiveness in predicting future LUCC trends in dynamic urban environments.

To predict desertification vulnerability in Jahun for the next 60 years, we analyzed annual LUCC changes between 2000 and 2020. The predicted LUCC images were meticulously aligned with the same coordinates and composition bounds as those used

http://www.aloki.hu ● ISSN 1589 1623 (Print) ● ISSN 1785 0037 (Online)
DOI: http://dx.doi.org/10.15666/aeer/2204_36413676

in the supervised classification, future projection, cross classification, and cubic trends analysis in Terrset. This alignment ensures accurate geographic data representation within the defined area, with coordinates spanning from Minimum X 431085, Maximum Y 501705, Minimum Y 1282335, to Maximum Y 1345455.

Desertification models

Geographic Information Systems (GIS) serve as essential instruments in compiling and overseeing extensive spatial databases. They conduct analyses to generate impactful visual presentations and management strategies. GIS plays a crucial part in the management and examination of digital geographic data, effectively conveying information visually, similar to traditional paper maps (Schreiber, 2013). Remote sensing involves acquiring information about objects or regions by measuring the radiation they reflect or emit from a distance (Campbell, 2006). It allows for the easy retrieval of images of areas at various points in time, offering a temporal perspective. Consistent coverage of an area through repeated imaging at different time intervals is crucial for applications like change detection (*Table 4*). Remote sensing systems, such as Modis and Landsat, can capture vast areas, providing comprehensive images of the desired area based on the needed resolution. Modeling desertification can be accomplished through simulation modeling and Geographic Information Systems or parametric methods. Simulation models offer detailed insights into environmental patterns and processes (Gharib, 2008)

Markov Chain Analysis Model (MCAM) serves as a stochastic framework utilized for simulating randomly evolving systems. It operates under the assumption that the current state dictates the future state, independent of the preceding sequence of events (Rabiner, 1989). MCAM represents a random process transitioning from one state to another, where the shift to the subsequent stage is solely determined by the current state, irrespective of the path leading to it, as depicted in *Figure 3.* Transition Probability Matrix encapsulates the likelihood of a cell transitioning from one land-use cover to another within a single time step, synthesized from classified image data.

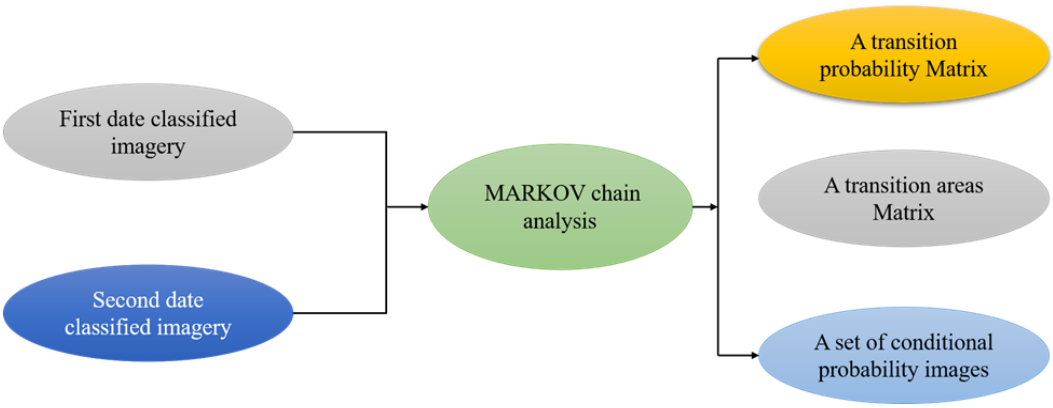

Figure 3. *Inputs and outputs of a Markov chain. (Source: El-hallaq and Habboub, 2015; Falaki et al., 2020)*

Markov models hold significant scientific appeal, serving as valuable tools for simulation exercises due to their mathematical rigor and foundation in empirical data (Monirsadat et al., 2011) Particularly noteworthy is the Cellular Automata Markov

http://www.aloki.hu ● ISSN 1589 1623 (Print) ● ISSN 1785 0037 (Online)
DOI: http://dx.doi.org/10.15666/aeer/2204_36413676

model, which effectively mirrors the dynamics of diverse natural and human systems. This model establishes a potent simulation framework represented by a spatial grid (raster), where a set of change rules dictates the attribute of each cell, considering neighboring cell characteristics. Its success stems from operational feasibility, user-friendliness, and the ability to articulate transition rules grounded in both logic and mathematics. Consequently, complex global patterns emerge directly from the application of simple local rules (White et al., 2001).

Results

Land use and land cover (LUCC) dynamics (Landsat imageries)

The analysis of Land Use and Land Cover (LUCC) dynamics over the years 2000, 2010, and 2020, as summarized in *Table 5*, reveals significant changes across different land cover categories. The total land area of 1172.1 km^2 remained constant over these years, suggesting that changes in individual land cover categories were offset by changes in others.

- Urban Land: In 2000, urban land covered 55.6 km^2, which decreased to 52.7 km^2 by 2010 and further to 42.1 km^2 in 2020. This represents a net decrease of 13.5 km^2 over 20 years.
- Vegetation: The area under vegetation was 104.7 km^2 in 2000, slightly decreasing to 103.7 km^2 in 2010, and then to 100.7 km^2 in 2020. Overall, there was a decrease of 4 km^2 in the vegetation-covered area from 2000 to 2020.
- Waterbodies: Covering 212.2 km^2 in 2000, waterbodies expanded to 255.1 km^2 in 2010, before slightly reducing to 237.8 km^2 in 2020. The net change from 2000 to 2020 was an increase of 25.5 km^2.
- Bare Lands: This category occupied 403.5 km^2 in 2000, decreased to 357.9 km^2 in 2010, and increased again to 383.1 km^2 in 2020. The overall change in bare lands over 20 years indicates a decrease of 20.4 km^2.
- Shallow Water: Initially covering 287.3 km^2 in 2000, shallow water areas increased to 303.3 km^2 in 2010 and further to 307.1 km^2 in 2020, resulting in a total increase of 19.7 km^2.
- Specialized Urban Areas: These areas covered 108.7 km^2 in 2000, decreased to 100.4 km^2 in 2010, and then slightly increased to 101.3 km^2 in 2020. This indicates a net decrease of 7.4 km^2 from 2000 to 2020 (*Fig. 4).*

The observed changes in these land cover categories reflect the dynamic nature of land use in the study area over the two decades.

Table 5. *Unsupervised land use land classification 2000-2020 to km^2*

LULC	2000	2010	2020	Changes
Urban	55.6	52.7	42.1	-13.5
Vegetation	104.7	103.7	100.7	-4
Waterbodies	212.2	255.1	237.8	25.6
Bare lands	403.5	357.9	383.1	-20.4
Shallow water	287.3	303.3	307.1	19.7
Specialized urban	108.7	100.4	101.3	-7.4
Total	1172.1	1172.1	1172.1	0

http://www.aloki.hu ● ISSN 1589 1623 (Print) ● ISSN 1785 0037 (Online)
DOI: http://dx.doi.org/10.15666/aeer/2204_36413676

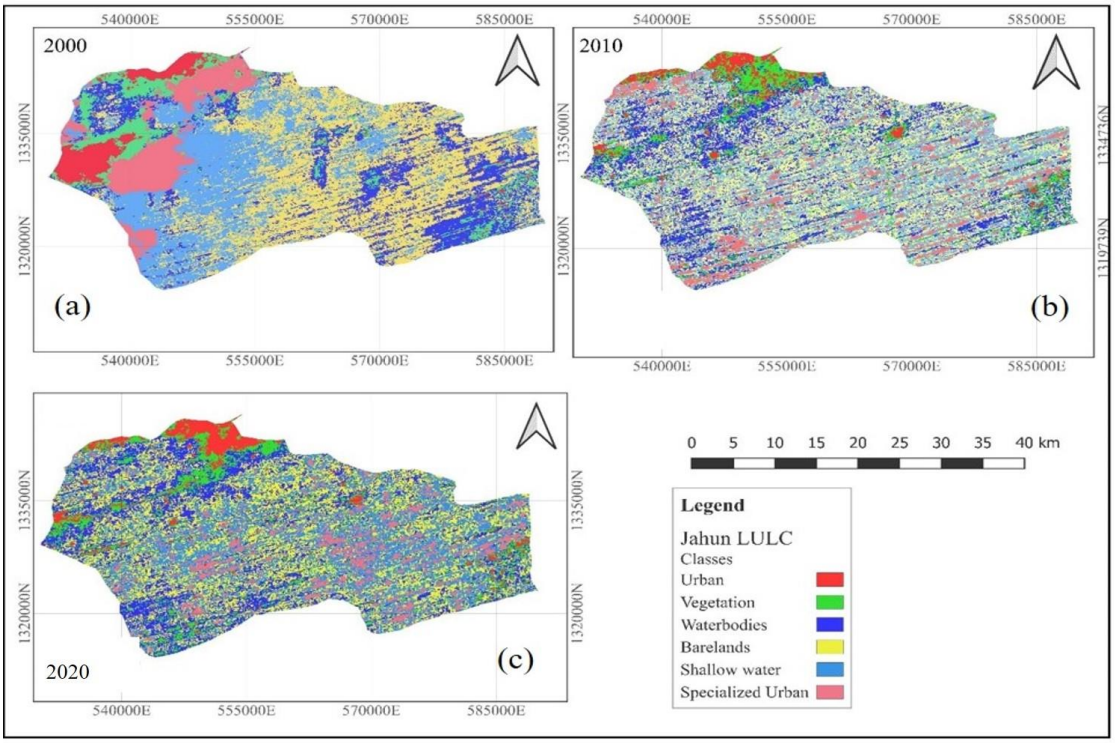

Figure 4. *Unsupervised land use and land cover change of the study area 2000-2020*

MODIS LULC dynamics

Cropland R/F (rainfed cropland)

Over the course of two decades, there was a notable decrease in the area covered by rainfed cropland, amounting to a significant reduction of approximately -34.41 km^2. This substantial decline in rainfed cropland suggests there may have been shifts in agricultural practices or changes in land-use policies within the region. In contrast, herbaceous cover exhibited a remarkable stability during this period, with only a minor decrease of about -0.42 km^2. This minimal change indicates that the extent of herbaceous vegetation in the area has remained largely unchanged. The post-flooding areas, interestingly, showed no change whatsoever. This consistency suggests that these areas have maintained a constant extent from 2000 to 2020, as depicted in *Figures 5*, *6*, and *7*. The observed dynamics in these specific land cover categories reflect nuanced changes in land use, particularly in agricultural and vegetative aspects of the region.

Figure 5 illustrates the MODIS land use and land cover changes in the study area for the year 2010. Key observations from this analysis include:

- Stability in Post-Flooding Areas: The post-flooding areas demonstrated remarkable stability, with no significant change observed. This consistency could be attributed to either consistent flood patterns or effective flood management practices in the region.
- Mosaic Cropland: There was a minor increase in mosaic cropland areas, approximately 0.55 km^2. This slight growth suggests some expansion or alteration in the distribution of cropland, possibly integrating a mix of other land covers.

http://www.aloki.hu ● ISSN 1589 1623 (Print) ● ISSN 1785 0037 (Online)
DOI: http://dx.doi.org/10.15666/aeer/2204_36413676

- Mosaic Natural Vegetation: The areas classified as mosaic natural vegetation remained unchanged over the two decades. The stability of natural vegetation in these mosaic areas may be due to successful conservation efforts or prevailing natural conditions that support the persistence of this vegetation type.
- Grassland Areas: A significant reduction was observed in grassland areas, with a decrease of about -35.85 km^2. This notable decrease suggests potential land conversion for other uses, such as urbanization or agriculture, which can have implications for local ecosystems.
- Urban Expansion: Urban areas witnessed a substantial increase, growing by approximately 1.89 km^2. This expansion highlights the ongoing urbanization trends in the region, likely driven by factors such as population growth and urban development.

Table 6 and *Figures 5*, *6*, and *7* provide further details on these land cover changes. The findings suggest a dynamic landscape undergoing various changes in land use, from natural vegetation and grasslands to urban development.

Table 6. *Spatio temporal land use land classification of the study area from 2000-2020 (Modis)*

S/N	Area_Sq_km	Class_2000	Area_Sq_km	Class_2010	Area_Sq_km	Class 2020	2000-2020	Change Area_Sq_km (2000-2020)
1.	710.10	Cropland R/F	735.77	Cropland R/F	744.51	Cropland R/F	Cropland R/F	-34.41
2.	23.62	Herbaceous cover	24.04	Herbaceous cover	24.04	Herbaceous cover	Herbaceous cover	-0.42
3.	12.99	Post-flooding	12.99	Post-flooding	12.99	Post-flooding	Post-flooding	0
4.	376.67	Mosaic cropland	376.86	Mosaic cropland	376.12	Mosaic cropland	Mosaic cropland	0.55
5.	12.89	Mosaic Nat Veg	12.89	Mosaic Nat Veg	12.89	Mosaic Nat Veg	Mosaic Nat Veg	0
6.	68.85	Grassland	42.69	Grassland	33.003	Grassland	Grassland	35.85
7.	0.19	Urban Areas	0.37	Urban Areas	2.07	Urban Areas	Urban Areas	-1.89

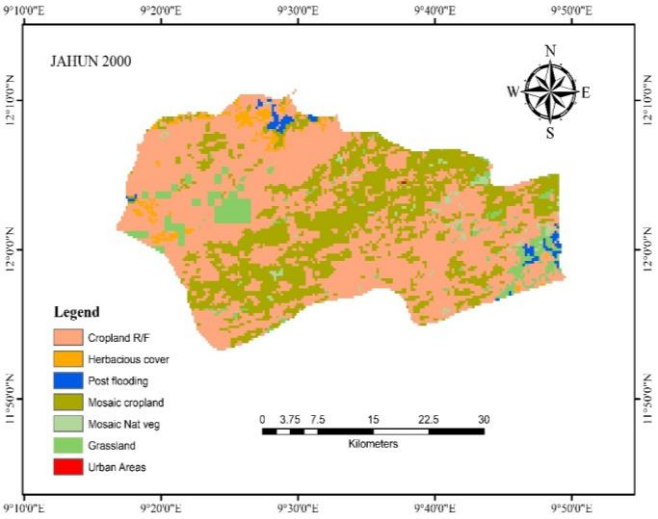

Figure 5. *Modis land use and land cover change of the study area 2000*

http://www.aloki.hu ● ISSN 1589 1623 (Print) ● ISSN 1785 0037 (Online)
DOI: http://dx.doi.org/10.15666/aeer/2204_36413676

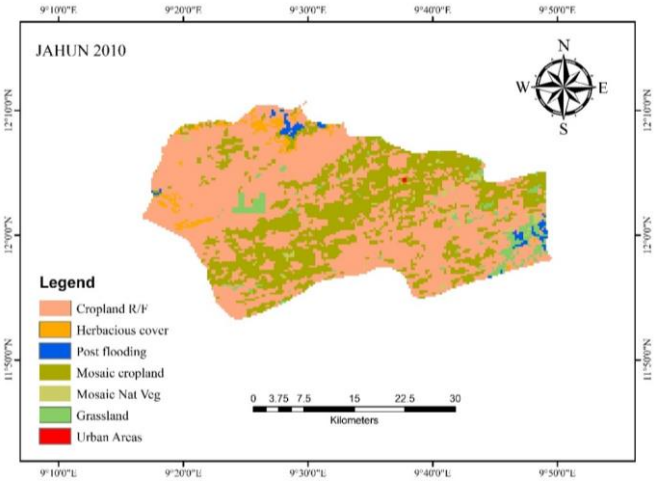

Figure 6. *Modis land use and land cover change of the study area 2010*

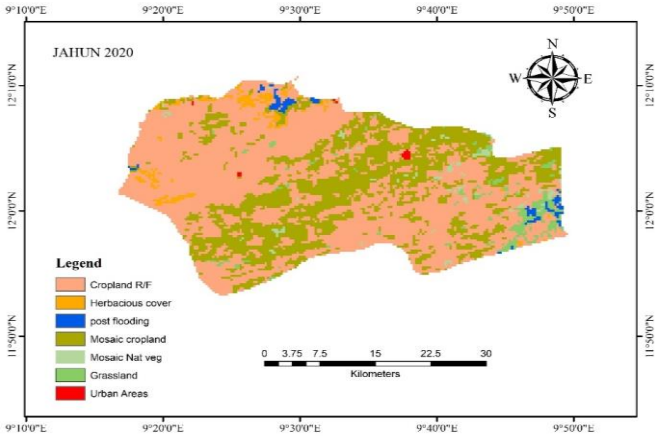

Figure 7. *Modis land use and land cover change of the study area 2020*

Maximum likelihood classification

The Maximum Likelihood Classification of the study area revealed notable changes in land use and land cover between 2000 and 2020:

- Urban Areas: In 2000, urban areas covered approximately 254.29 km^2. By 2020, this had significantly reduced to about 115.62 km^2. This substantial reduction suggests possible shifts in urban development patterns or changes in land-use policies, potentially leading to the conversion of urban land into other uses.
- Vegetation: The area occupied by vegetation also showed a decrease, from about 366.95 km^2 in 2000 to approximately 160.62 km^2 in 2020. This decline could indicate deforestation or changes in land cover due to factors like agricultural expansion or urbanization.
- Waterbodies: These areas remained relatively stable, with a slight increase from approximately 7.19 km^2 in 2000 to about 8.20 km^2 in 2020. The stability, with a minor increase, might be a result of natural variations or changes in water management practices.

http://www.aloki.hu ● ISSN 1589 1623 (Print) ● ISSN 1785 0037 (Online)
DOI: http://dx.doi.org/10.15666/aeer/2204_36413676

- Bare Lands: Contrasting with the decrease in urban and vegetated areas, bare lands expanded notably from 148.20 km^2 in 2000 to about 499.19 km^2 in 2020. This significant increase could be attributed to various factors, including land conversion for agriculture, urbanization, or natural land degradation processes.

Table 7 provides detailed statistics of these changes, while *Figure 8* illustrates the spatial distribution of these land cover transitions. The observed changes highlight a dynamic landscape undergoing various transformations, reflecting the interplay of environmental, urban, and agricultural factors over the two decades.

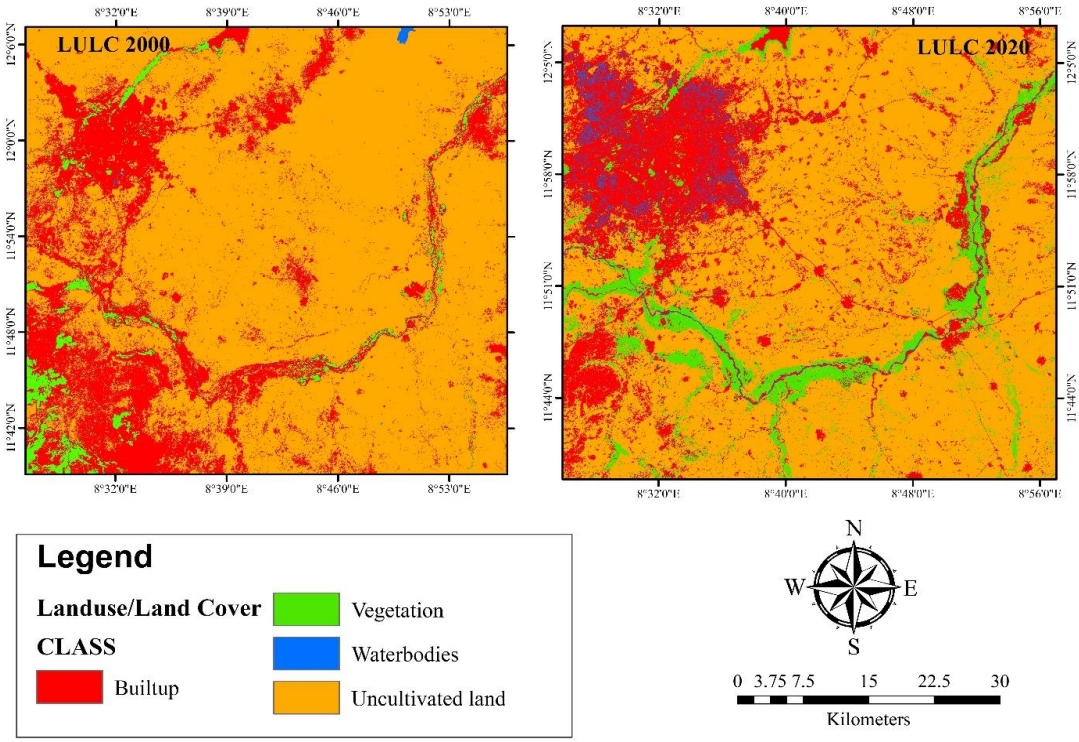

Figure 8. *Supervised land use and land cover change of the study area 2000 and 2020*

Table 7. *Spatio-temporal land use/land cover classification of the study area from 2000 to 2020 (Landsat)*

Class 2000	Square km	Square km	Class 2020	Changes
Urban areas	254.2869	115.6212	Urban Areas	-138.6657
Vegetation	366.948	160.6158	Vegetation	-206.3322
Waterbodies	7.1928	1.2015	Waterbodies	-5.9913
Bare lands	148.1976	499.1868	Bare lands	350.9892
Total	776.63	776.63	Total	0

Some inconsistencies were noted, particularly in *Tables 5* and *7*, specifically regarding parameter values for Urban Areas with areas of 55 km² and 254 km², respectively. This variance stems from the different classification techniques employed in each table. In *Table 5*, we utilized unsupervised classification techniques where the pixel selection was automated by software such as ENVI, ArcMap, etc. Conversely, in

http://www.aloki.hu ● ISSN 1589 1623 (Print) ● ISSN 1785 0037 (Online)
DOI: http://dx.doi.org/10.15666/aeer/2204_36413676

Table 7, we employed supervised classification techniques, allowing us to manually select parameters, as outlined in *Tables 1–3*, respectively. Numerous scholars have found supervised classification to be more reliable and convincing in Land Use and Land Cover Change (LUCC) analysis, as evidenced by studies such as those by Routh et al. (2018) and Muñoz-Marí et al. (2007)

Hence, we utilized data from the supervised classification technique to forecast future desertification patterns in Jahun, Jigawa State, as depicted in *Figure 10* and *Table 11*.

From 2000 to 2020, the study area experienced notable shifts in land cover. Urban areas saw a significant reduction, decreasing by approximately 138.67 km^2. This change suggests a potential shift away from urban development or alterations in land-use policies, leading to the conversion of urban land into other categories. Concurrently, the area covered by vegetation also witnessed a decline of about 206.33 km^2, pointing towards potential deforestation or land cover changes driven by agricultural expansion or urbanization. In contrast, waterbodies exhibited relative stability, with a slight increase of approximately 1.01 km^2. This minor change could be attributed to natural fluctuations or evolving water management practices. Meanwhile, bare lands experienced a substantial increase, expanding by around 350.99 km^2. This expansion indicates significant land conversion, possibly for agricultural purposes, urban development, or as a result of natural land degradation processes.

Overall, the two-decade period under study saw marked transformations in land cover, characterized by reductions in urban and vegetated areas, a marginal increase in waterbodies, and a notable expansion in bare lands. These changes likely reflect complex interactions of various factors including urbanization, agriculture, and environmental dynamics. Further research is necessary to fully understand the underlying drivers and potential implications of these land cover shifts.

Cross-classification results for land cover classification

In this section, we interpret the cross-classification results derived from the Maximum Likelihood classification method applied to land cover data from 2000 and 2020, as illustrated in *Figure 9*. The classification categorized land cover into four classes: Urban, Vegetation, Waterbodies, and Uncultivated Land. The results, presented in a confusion matrix format (*Table 8*), offer insights into the classification model's accuracy and performance.

Let us examine how land was classified in each category:

(A) True category: urban

- Urban Classified as Urban: Approximately 308.58 km^2 were correctly identified as urban, demonstrating a high accuracy in urban area classification.
- Urban Classified as Vegetation: Around 75.24 km^2 of urban areas were mistakenly classified as vegetation, possibly due to the presence of vegetated areas like urban parks or green spaces within urban zones.
- Urban Classified as Waterbodies: A small area, about 3.14 km^2, of urban land was incorrectly classified as waterbodies, likely representing water features within urban settings.
- Urban Classified as Uncultivated Land: A significant portion, approximately 452.71 km^2, of urban land was misclassified as uncultivated. This misclassification might be attributed to urban areas with sparse development or open spaces that resemble uncultivated land.

http://www.aloki.hu ● ISSN 1589 1623 (Print) ● ISSN 1785 0037 (Online)
DOI: http://dx.doi.org/10.15666/aeer/2204_36413676

Each cell in the confusion matrix (*Table 8*) represents the area in square kilometers that was classified as a particular category, based on the actual land cover type. This approach provides a detailed view of the classification accuracy for each land cover type.

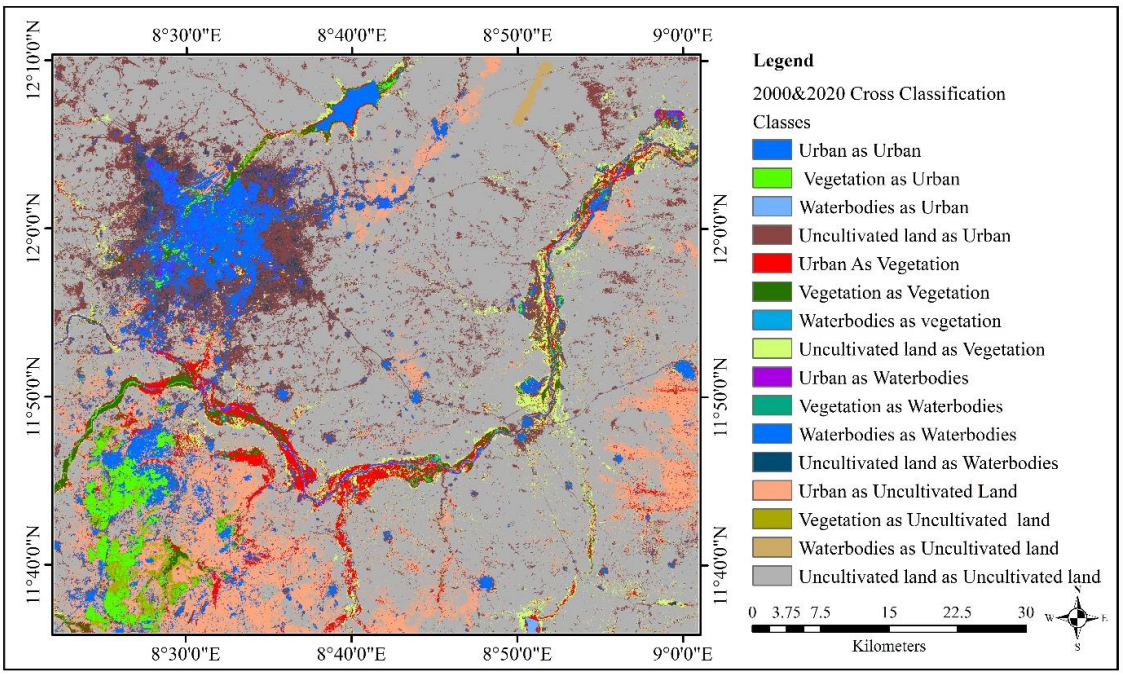

Figure 9. *Cross-classification results of the study area 2000-2020*

Table 8. *Cross-classification results of the confusion matrix for each class over the years 2000-2020*

Category	Hectares	Legend
1	6722.19	1 | 1
2	4294.71	2 | 1
3	434.52	3 | 1
4	110.7	4 | 1
5	1569.33	1 | 2
6	11238.12	2 | 2
7	127.08	3 | 2
8	3127.05	4 | 2
9	39.24	1 | 3
10	14.22	2 | 3
11	51.57	3 | 3
12	15.12	4 | 3
13	17097.93	1 | 4
14	21147.75	2 | 4
15	106.11	3 | 4
16	11566.89	4 | 4

http://www.aloki.hu ● ISSN 1589 1623 (Print) ● ISSN 1785 0037 (Online)
DOI: http://dx.doi.org/10.15666/aeer/2204_36413676

(B) True category: vegetation

- Vegetation Classified as Urban: Approximately 155.46 km^2 of vegetation were misclassified as urban, possibly due to dense vegetation in residential areas or misidentified cultivated landscapes.
- Vegetation Classified as Vegetation: A significant 53.97 km^2 of vegetation were correctly identified, demonstrating the classification's reliability in recognizing vegetated areas.
- Vegetation Classified as Waterbodies: Only a minor area, about 0.25 km^2, was incorrectly classified as waterbodies, likely corresponding to vegetation along water edges.
- Vegetation Classified as Uncultivated Land: Around 143.90 km^2 of vegetation areas were misclassified as uncultivated land, potentially due to sparse vegetation or challenging spectral signatures.

(C) True category: waterbodies

- Waterbodies Classified as Urban: A small area of 22.73 km^2 of waterbodies was misclassified as urban, possibly representing built-up areas near water.
- Waterbodies Classified as Vegetation: Only 1.08 km^2 of waterbodies were inaccurately classified as vegetation, likely due to aquatic vegetation.
- Waterbodies Classified as Waterbodies: A mere 0.97 km^2 of waterbodies were correctly classified, suggesting challenges in accurately classifying complex water bodies.
- Waterbodies Classified as Uncultivated Land: About 31.00 km^2 were mistakenly classified as uncultivated land, possibly due to spectral similarities between open water and certain land types.

(D) True category: uncultivated land

- Uncultivated Land Classified as Urban: A significant 481.08 km^2 of uncultivated land were incorrectly classified as urban, potentially due to sparse urbanization in these areas.
- Uncultivated Land Classified as Vegetation: Roughly 43.46 km^2 were misclassified as vegetation, likely because of natural vegetation in these areas.
- Uncultivated Land Classified as Waterbodies: About 7.99 km^2 of uncultivated land were inaccurately classified as waterbodies, perhaps due to proximity to water bodies.
- Uncultivated Land Classified as Uncultivated Land: A substantial 2675.97 km^2 were correctly identified as uncultivated land, indicating good performance of the classification method in this category.

These cross-classification results provide a detailed understanding of the classification accuracy for each land cover category, highlighting both the successes and challenges of the Maximum Likelihood classification method used in the study. In our analysis, we projected changes in land cover up to the year 2080 by categorizing the landscape into four distinct classes: Class 1, Class 2, Class 3, and Class 4. These classifications represent specific types of land cover, crucial for understanding landscape dynamics over time. The projection data is summarized in a probability table (*Table 9*), which shows the likelihood of transition between these classes. The

http://www.aloki.hu ● ISSN 1589 1623 (Print) ● ISSN 1785 0037 (Online)
DOI: http://dx.doi.org/10.15666/aeer/2204_36413676

probabilities range from 0.0010 to 0.7356, indicating the chances of each land cover class transitioning to another over the specified time interval.

Projection

Table 9. *Projection probability table of changing to Cl. 1 Cl. 2 Cl. 3 Cl. 4*

Classes	CL. 1	CL. 2	CL. 3	CL. 4
Class 1	0.0554	0.2080	0.0011	0.7356
Class 2	0.0548	0.2214	0.0010	0.7227
Class 3	0.1115	0.1780	0.0024	0.7081
Class 4	0.0401	0.2284	0.0010	0.7306

For instance:

At the intersection of "Class 1" and "Cl. 2," the value 0.2080 suggests a 20.80% probability that land cover in Class 1 will change to Class 2. This indicates a notable likelihood of this type of land cover transition occurring by 2080. Similarly, the value 0.1115 at the intersection of "Class 3" and "Cl. 1" reflects an 11.15% chance that land cover in Class 3 will transition to Class 1.

These probabilities are essential for anticipating how the land cover might evolve in the future. They provide insights crucial for planning and managing land use, especially in areas where significant environmental changes are expected.

Temporal context and projection parameters

This part of our analysis focuses on understanding the temporal context and key parameters that frame our land cover change projections.

(i) output prefix and time intervals

- Output Prefix: The output prefix "2080_JAHUN" indicates that the projections are intended to represent the year 2080. This helps in identifying the specific target year for our land cover change predictions.
- Time Interval 1: The first-time interval, marked as 20 years, refers to the period from 2000 to 2020. This interval provides the baseline for assessing changes in land cover over these two decades.
- Time Interval 2: The second time interval is set at 60 years, extending the projection to a longer term. This suggests an analysis that encompasses the changes from 2020 through to 2080, offering a more comprehensive view of potential long-term land cover dynamics.

(ii) Background cell option and proportional error

- Background Cell Option: This parameter is related to the modelling or analysis process but is not detailed in the given context.
- Proportional Error: The proportional error being set to 0.0 implies that the model does not incorporate any error or uncertainty in the probability values. While this simplifies the model, it is important to note that in reality, projections often entail some degree of uncertainty.

In summary, this projection data is crucial for modelling or predicting land cover changes, particularly relevant to fields like environmental science, geography, or land

http://www.aloki.hu ● ISSN 1589 1623 (Print) ● ISSN 1785 0037 (Online)
DOI: http://dx.doi.org/10.15666/aeer/2204_36413676

use planning. The insights gained into how different land cover classes may evolve over time are valuable for informed decision-making in land management and resource allocation. However, the absence of proportional error in the model suggests that these probabilities are presented as precise estimates, without accounting for potential uncertainties inherent in long-term projections.

2080 prediction: (2000–2020)

The land cover prediction for the year 2080, based on data from 2000, indicates significant changes in various categories:

- Urban Areas: Urban regions are expected to undergo a considerable decrease to about 110.86 km^2. This substantial decline points towards a potential reversal in urban expansion trends or alterations in urban development strategies. The predicted reduction suggests a shift away from urbanization, possibly due to changes in demographic trends, economic factors, or land-use policies.
- Vegetation: The area covered by vegetation is projected to decrease to approximately 247.94 km^2. This notable decline indicates potential deforestation or changes in land use that adversely affect natural vegetation. It could be driven by factors such as agricultural expansion, urban development, or environmental changes.
- Waterbodies: Waterbodies are expected to see a slight increase, reaching around 1.07 km^2. This minor change could result from natural fluctuations in water bodies or the effects of water management practices. The stability of waterbodies suggests balanced management or the resilience of these ecosystems to change.
- Bare Lands: A significant expansion in bare lands is anticipated, with the area increasing to about 416.75 km^2. This expansion suggests considerable land conversion, potentially for agricultural use, urban development, or as a consequence of natural land degradation processes.

Figure 10A provides a visual representation of these projected changes. The anticipated trends in land cover by 2080 highlight the dynamic nature of land use and the importance of considering these changes in future planning and environmental management strategies.

2080 Prediction1: (2020–2080)

This second projection for 2080, taking 2020 as the baseline, mirrors the trends observed in the first projection:

- Urban areas: There is an expected significant reduction in urban areas, with the area decreasing to approximately 110.86 km^2. This consistent prediction in both projections underlines a potential trend of diminishing urbanization.
- Vegetation: Similarly, vegetation cover is projected to decrease to about 247.94 km^2. This decline, observed in both projections, suggests ongoing deforestation or land use changes impacting natural vegetation.
- Waterbodies: In line with the first projection, waterbodies are expected to experience a minor increase, reaching approximately 1.07 km^2. The stability of waterbodies across both projections indicates minimal changes in this category.

http://www.aloki.hu ● ISSN 1589 1623 (Print) ● ISSN 1785 0037 (Online)
DOI: http://dx.doi.org/10.15666/aeer/2204_36413676

- Bare lands: The expansion of bare lands is anticipated to be substantial, with an increase to about 416.75 km^2, mirroring the first projection's findings.

These projections, as depicted in *Figure 10B*, indicate a consistent trend across both timeframes, characterized by reduced urban areas, decreased vegetation, and increased bare lands by the year 2080. Waterbodies, however, are projected to remain relatively stable. These trends suggest that factors such as urbanization, land-use policies, climate, and environmental conditions could be influencing these changes (*Table 10*).

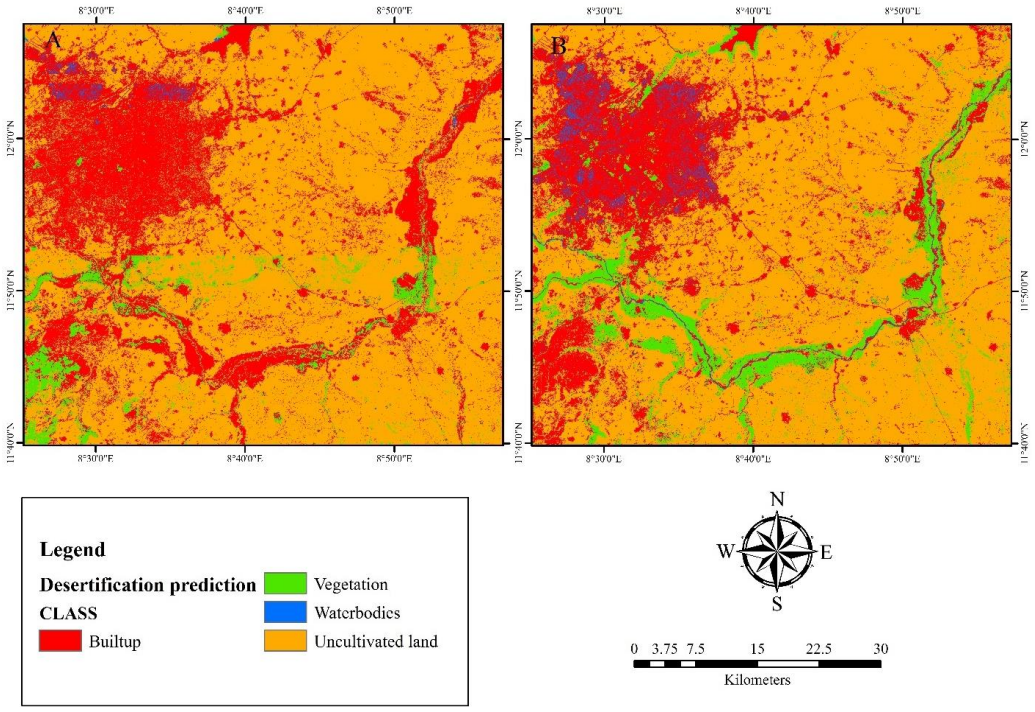

Figure 10. *Desertification prediction map of the study area: (A) 2000-2080, (B) desertification prediction map of the study area: 2020-2080*

Table 10. *Projection of the study area from 2000 to 2080 and 2020 to 2080*

S/NO	Area_Sq_km	2080_Prediction	Area_Sq_km	2080_Prediction 1
1	237.6981	Urban area	110.8611	Urban area
2	473.1111	Vegetation	247.9446	Vegetation
3	6.39	Waterbodies	1.0665	Waterbodies
4	59.4261	Bare lands	416.7523	Bare lands

Gain and loss in land cover categories (2000–2020)

This part of the analysis, illustrated in *Figure 11*, details the gains and losses experienced in various land cover categories over a 20-year period:

(i) Built-up areas

- Gain: There was a significant increase in built-up areas, with a gain of approximately 590,102 units (square meters or hectares), indicating substantial urban or infrastructure development.

http://www.aloki.hu ● ISSN 1589 1623 (Print) ● ISSN 1785 0037 (Online)
DOI: http://dx.doi.org/10.15666/aeer/2204_36413676

- Loss: Conversely, there was also a notable loss of built-up areas, amounting to approximately -732,515 units. This reduction could be due to urban redevelopment, demolitions, or shifts in land use policies.

(ii) Vegetation

- Gain: Vegetation saw a notable gain of approximately 332,895 units, which could be attributed to reforestation efforts, afforestation programs, or natural vegetation regrowth.
- Loss: Conversely, the loss in vegetation was approximately -133,100 units, potentially due to deforestation, agricultural expansion, or other land use changes.

(iii) Waterbodies

- Gain: Waterbodies experienced an increase of about 60,903 units, suggesting an expansion of water features influenced by natural factors like precipitation or water management practices.
- Loss: There was a decrease of approximately -12,650 units in waterbodies, possibly due to the construction of water reservoirs, drought conditions, or alterations in river courses.

(iv) Uncultivated land

- Gain: Uncultivated land saw a gain of about 591,708 units, possibly due to land being set aside for conservation, rewilding, or abandonment of agricultural fields.
- Loss: There was a loss of approximately -697,343 units in uncultivated land, indicating a reduction in unused or natural land, likely due to agricultural expansion or urbanization.

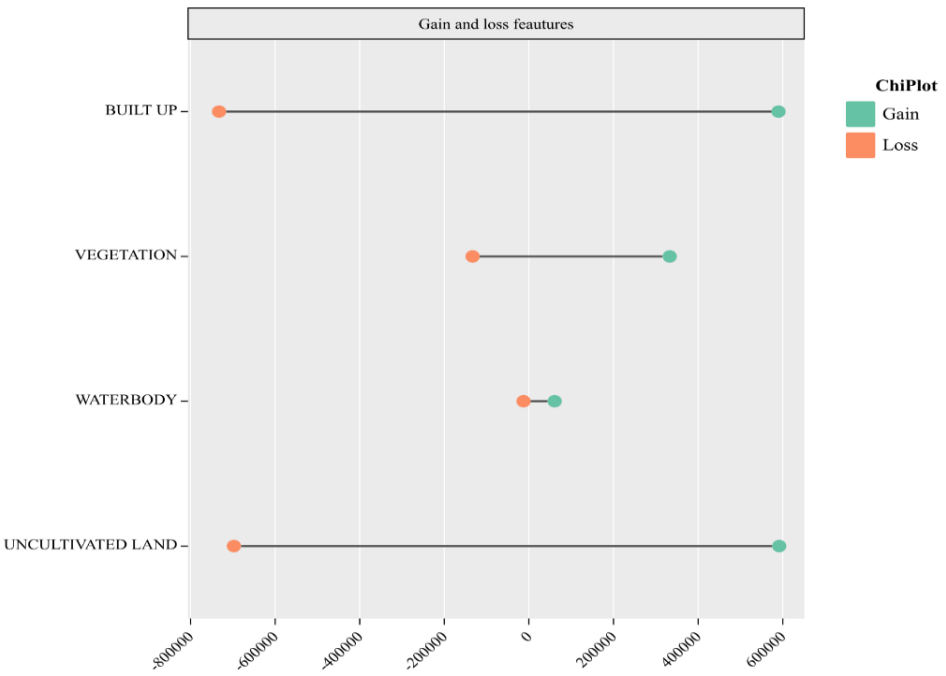

Figure 11. *Features gain and loss of the study area 2000-2020*

http://www.aloki.hu ● ISSN 1589 1623 (Print) ● ISSN 1785 0037 (Online)
DOI: http://dx.doi.org/10.15666/aeer/2204_36413676

Figure 11 visually represents these changes in land cover categories. The data underscores significant transformations in the landscape, reflecting the complex interplay between natural processes and human activities in shaping land use patterns.

Magnitude and rate of desertification (2000–2020)

Table 11 provides a comprehensive overview of the changes in various land cover categories within the study area over a span of 20 years, offering critical insights into the dynamics of desertification:

- Urban areas: Experienced a decrease of 138.6657 km^2 from 2000 to 2020. This change amounts to a rate of 6.3030 km^2/year, equating to a 54.55% reduction over the two decades.
- Vegetation: Saw a reduction of 206.3322 km^2, with an annual rate of change of 9.3787 km^2. This represents a significant decline of about 56.25% during this period.
- Waterbodies: Exhibited a substantial decrease of 5.9913 km^2, at a rate of 0.2723 km^2 per year, amounting to an 83.33% reduction.
- Bare Lands: Showed a dramatic increase of 350.9892 km^2, with an annual change rate of 15.9541 km^2, reflecting a significant expansion of approximately 236.79%.

Table 11. *Magnitude and rate of desertification between 2000 and 2020*

Category	Class 2000 (km^2)	Class 2020 (km^2)	Extent of change (km^2)	Rate of change (km^2/year)	Rate of change (%/year)
Urban areas	254.2869	115.6212	138.6657	6.3030	54.55%
Vegetation	366.948	160.6158	206.3322	9.3787	56.25%
Waterbodies	7.1928	1.2015	5.9913	0.2723	83.33%
Bare lands	148.1976	499.1868	350.9892	15.9541	236.79%

The magnitude represents the absolute value of the extent of change, measuring the size of the change irrespective of whether it is an increase or decrease. Hence, the change is always a positive or zero value, indicating the scale of land cover change between the initial and final years, regardless of the direction of the change.

Spatial trend of change

Cubic trends: vegetation to build-up areas

In landscapes significantly influenced by human activities, the patterns of change are often complex, as noted by Hamdy et al. (2017). This complexity is especially evident when examining the transitions between vegetation and built-up areas.

Modelling change with cubic trends

- Initial Phase (Decrease in Vegetation): The model begins with negative values (-0.03, -0.01), indicating a decline in vegetation. This trend suggests an initial period where vegetated areas are diminishing, potentially due to factors like urban expansion or land use changes.

http://www.aloki.hu ● ISSN 1589 1623 (Print) ● ISSN 1785 0037 (Online)
DOI: http://dx.doi.org/10.15666/aeer/2204_36413676

- Middle Phase (Transition Period): As the values shift from -0.01 to 0.01, there is a noticeable transition towards positive values. This indicates a potential slowing down or reversal of the decrease in vegetation. This period might represent a turning point where factors contributing to vegetation loss are mitigated or reversed.
- Final Phase (Increase in Vegetation): From 0.01 to 0.23, the values steadily climb, signifying a gradual recovery or growth in vegetation areas. This positive trend might be due to improved environmental conditions or successful reforestation efforts.

The cubic trend highlights that the rate of change in vegetation cover is not linear. It accelerates during the transition from negative to positive values and continues to increase during the positive phase. This non-linear pattern suggests that the drivers behind vegetation change are dynamic and evolve over time.

Relationship with built-up areas

Inversely, as vegetation areas decrease, built-up areas might expand, reflecting urbanization trends. Conversely, as vegetation starts to recover, the expansion of built-up areas might slow down or decrease. The cubic trend can be instrumental in pinpointing periods of rapid urbanization, marked by significant increases in built-up areas, which often coincide with periods of vegetation loss. Subsequent periods of vegetation recovery might correlate with a stabilization or reduction in urban expansion. *Figure 12* illustrates these trends and transitions, providing a visual representation of the complex interplay between urbanization and vegetation change over time.

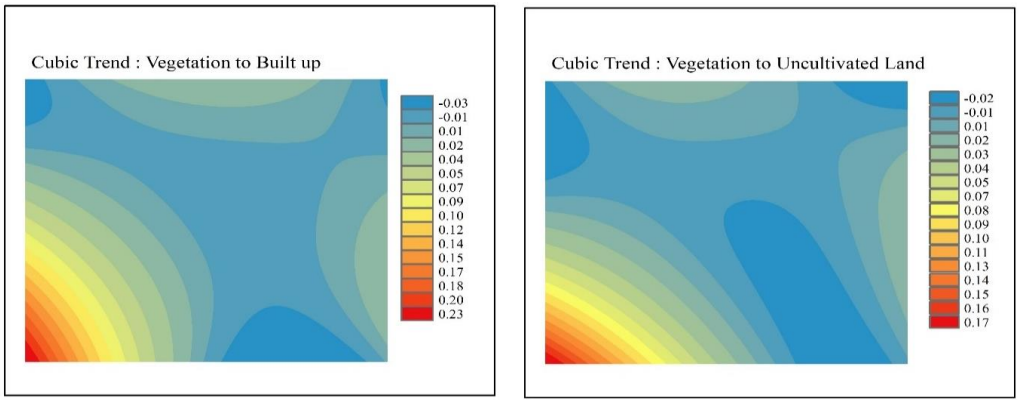

Figure 12. *Map of cubic trends of the study area*

Cubic trends: vegetation to uncultivated land

The analysis of cubic trends provides insights into the dynamic relationship between vegetation and uncultivated land. This trend is particularly useful in understanding how changes in one category impact the other over time.

Modelling change with cubic trends

- Initial Phase (Decrease in Vegetation): The model starts with negative values (-0.02, -0.01), indicating a reduction in vegetation. This phase likely represents a

http://www.aloki.hu ● ISSN 1589 1623 (Print) ● ISSN 1785 0037 (Online)
DOI: http://dx.doi.org/10.15666/aeer/2204_36413676

period where vegetated areas are declining, possibly due to various environmental or anthropogenic factors.

- Middle Phase (Transition Period): As the trend progresses, values shift from -0.01 to 0.17, moving towards positive numbers. This change suggests a possible slowing or reversal of the decrease in vegetation. This turning point might be attributable to improved environmental conditions or effective land management practices.
- Final Phase (Increase in Vegetation): Beyond 0.17, the values continue to rise, indicating a gradual recovery or increase in vegetation. This positive trend could be a result of favorable conditions leading to vegetation growth or successful restoration efforts.

Inverse relationship with uncultivated land

In this relationship, an inverse trend is observed: as vegetation decreases, uncultivated land may increase, and vice versa. As vegetative areas diminish, it could lead to an expansion in uncultivated land, reflecting changes in land use or abandonment of cultivated areas. Conversely, as vegetation begins to recover and expand, uncultivated land may decrease, suggesting a shift towards more active land use or reforestation.

Discussion

Land cover refers to the physical cover of the Earth's surface, while land use pertains to how humans utilize this land (Chen et al., 2018; Afrin et al., 2019). The rapid transformation of land cover/land use (LUCC) is a strong indicator of global climate change (Prasad et al., 2022). Previous research has explored comparing different satellite sensors for LUCC classification (Chander et al., 2008; Deng et al., 2008; Ghayour et al., 2021).

Accessing land use landcover using different satellites

In our study, we utilized various satellites to assess the true LUCC of our study area. Landsat offers a resolution of 30 m, whereas MODIS provides a resolution of 500 m. This difference in resolution is evident in the slight discrepancies observed in LUCC variables across (*Figs. 4–7)*. These variations are attributable to the satellites' resolution capabilities, the pixels captured, and the classification techniques employed. However, the critical aspect of our analysis is monitoring desertification risk by incorporating data from two Landsat satellites and employing three different classification techniques, as illustrated in *Figures 4–8*. The relationships among variables in *Tables 5–7* underscore the complexities and variabilities in LUCC change from 2000 to 2020. While all tables consistently show decreased vegetation, other categories exhibit discrepancies due to different data sources and methodologies. Urban areas show a decrease in *Tables 5* and *7* but an increase in *Table 6*, likely reflecting variations in MODIS and Landsat data classifications or resolutions. Similarly, waterbodies increase in *Table 5* but decrease in *Table 7*, a divergence possibly stemming from different spatial resolutions and classification methods. Bare lands increase in *Table 7* but decrease in *Table 5*, suggesting diverse impacts of land conversion or degradation. Despite these variations,

http://www.aloki.hu ● ISSN 1589 1623 (Print) ● ISSN 1785 0037 (Online)
DOI: http://dx.doi.org/10.15666/aeer/2204_36413676

the total land area remains constant, indicating changes in land cover types rather than physical land alterations.

These findings highlight the importance of considering methodological differences when interpreting LUCC data for accurate environmental planning and decision-making. Challenges such as multi-source, multi-temporal, and multi-level analysis, along with concerns about robustness, quality, and scalability, remain pivotal areas for further study in remote sensing (Macarringue et al., 2022).

Desertification prediction

Following the insights from our land use and land cover (LUCC) analysis of the study area, we employed the Markov chain model to forecast future desertification trends. The Markov chain model, noted for its efficacy in various environmental sustainability studies, provides a robust framework for such predictions. Verma et al. (2024) successfully applied this model for mapping forest carbon sequestration in the Western Himalaya, while Pechanec et al. (2018) utilized it for carbon sequestration prediction under climate change scenarios. Drawing inspiration from these applications and the minimal error intervention associated with the Markov chain analysis, we integrated this model to predict the trajectory of desertification in Jahun, Jigawa State.

Our research, while primarily focusing on vegetation, built-up areas, waterbodies, and bare lands, also elucidates the probability of land cover transitioning from one category to another. It highlights the gains and losses in these LUCC variables over a two-decade period. The accuracy of our analysis is further substantiated by the cross-classification results and the confusion matrix presented for each LUCC variable (*Fig. 9; Table 8*).

The inhabitants of the study area, predominantly engaged in farming activities, are increasingly impacted by the encroachment of desertification and the broader challenges posed by global climate change and economic factors. These influences are affecting agricultural output and precipitation patterns, necessitating a detailed analysis and prediction of LUCC changes. Our risk assessment aims to inform government policymakers and urban planners, providing crucial data to safeguard the future of one of Jigawa State's oldest local governments.

Given the limited number of research articles specific to our study area, we have endeavored to compare our findings with those from neighboring states or locations with similar morphological and climatic features. This comparative approach enhances the relevance and applicability of our results in broader environmental and socio-economic contexts. In this discussion, we offer a comprehensive overview of our findings, drawing upon prior research to present a holistic understanding of the dynamics of desertification and their extensive implications. Our study reveals a significant decline in urban areas, highlighting the rapid transformation of landscapes. This phenomenon may be linked to recurrent flooding in the area, as documented by Tudunwada (2022). Muhammad (2020) identified persistent flooding in Dutse municipality, Jigawa State, Nigeria, as a major environmental hazard. The concurrent reduction in vegetation cover in our study aligns with observations by Mohammed et al. (2020) emphasizing the ecological challenges posed by diminishing vegetation. This trend underscores the need for urgent interventions like afforestation and reforestation, as recommended by Ibrahim et al. (2023) to preserve fragile ecosystems.

A notable finding from our research is the rapid expansion of bare lands, as seen in *Figures 4–7,* a trend consistent with findings by Zangina et al. (2019). The observed

http://www.aloki.hu ● ISSN 1589 1623 (Print) ● ISSN 1785 0037 (Online)
DOI: http://dx.doi.org/10.15666/aeer/2204_36413676

reduction in waterbodies, analyzed through supervised classification in Idrisi Terrset, stresses the importance of water resource conservation, particularly in light of increasing water scarcity in arid regions. Our projections of desertification vulnerability phases from 2000 to 2080 and 2020 to 2080, modelled using Idrisi Terrset, align with the methodologies employed by Falaki et al. (2020) in Jibia and Tariq et al. (2022) in Peshawar, Pakistan. These projections offer valuable insights for policymakers, planners, and government agencies. The cross-classification results presented in *Figure 9* and *Table 8* not only demonstrate the accuracy and effectiveness of our classification model but also reveal dynamic changes in the net gain and loss across the study area's four main classes.

Our research highlights a significant decrease in urban areas and vegetation, coupled with an increase in uncultivated land. This finding is echoed in studies like that of Koko et al. (2022) in Kano State, which shares similar terrain and climatic conditions with Jigawa Jahun. Their work reported a substantial increase in built-up areas, underscoring the need for sustainable urban planning.

In summary, our study enhances the understanding of desertification dynamics in Jahun Local Government Area. By integrating prior studies and employing advanced classification techniques, we illuminate the multifaceted challenges and the need for urgent interventions to mitigate the adverse effects of desertification. Our findings reveal significant changes in land cover and environmental dynamics from 2000 to 2020, with substantial decreases in urban areas and vegetation, and an increase in bare lands. The reduction in waterbodies further highlights the importance of conserving water resources in arid regions facing scarcity. The projections of desertification vulnerability provide critical insights for future planning and emphasize the necessity of sustainable urban planning and land use policies to effectively combat land degradation.

Limitations

Our study on desertification in the Jahun Local Government Area encountered several limitations. The utilization of MODIS data, characterized by lower spatial resolution, potentially hindered our ability to detect fine-scale land cover changes accurately. Moreover, our focus on the timeframe from 2000 to 2020 may have overlooked longer-term trends in desertification dynamics. Additionally, our reliance on remotely sensed data and supervised classification methods may have introduced inaccuracies, emphasizing the need for ground validation to enhance the study's reliability. Furthermore, our analysis did not fully explore the influences of climate factors, policy decisions, or socio-economic factors on desertification processes. It is important to note that while our findings provide valuable insights, they are context-specific to the study area and may not be directly transferable to regions with differing environmental and socio-economic conditions. For future research, incorporating advanced modeling techniques and extensive field validation could enhance the accuracy and reliability of desertification assessments.

Conclusions

Our study in Jahun Local Government Area, Jigawa State, Nigeria, addresses the critical environmental challenge of desertification. Employing Cellular Automata Markov Chain Analysis, we aimed to assess and predict desertification risks up to 2080.

http://www.aloki.hu ● ISSN 1589 1623 (Print) ● ISSN 1785 0037 (Online)
DOI: http://dx.doi.org/10.15666/aeer/2204_36413676

Our approach integrated unsupervised Landsat classification, MODIS-based LUCC analysis, Maximum Likelihood classification through Idrisi Terrset, and cubic trend analysis. The findings indicate substantial land cover transformations, including a significant reduction in urban areas and vegetation, a decrease in waterbodies, and an alarming expansion of bare lands. These results contribute valuable insights into the complex dynamics of desertification in the region, highlighting areas at high risk of environmental degradation.

Recommendations

1. Integrated Monitoring and Management: Implement an integrated monitoring and management approach that combines remote sensing technologies and Geographic Information Systems (GIS) to track land cover changes and desertification trends. Continuous monitoring will enable timely intervention.
2. Rural Development: Invest in rural development programs that promote sustainable land use practices, afforestation, and soil conservation techniques. These efforts will help mitigate the expansion of bare lands and protect vital ecosystems.
3. Community Engagement: Foster community engagement and awareness regarding the consequences of desertification. Empower local communities to actively participate in desertification mitigation through community-based projects and education.
4. Policy and Regulation: Develop and enforce land use policies and regulations that encourage responsible land management. This includes measures to control urban sprawl and promote sustainable urban planning.
5. Research and Innovation: Support ongoing research and innovation in desertification monitoring and mitigation. Collaborate with academic institutions and research organizations to explore innovative solutions.
6. International Cooperation: Collaborate with neighboring regions and international bodies to address cross-border desertification challenges. Desertification often transcends political boundaries and requires collaborative efforts.

Acknowledgments. The authors wish to thank the Integration and application of appropriate technologies for desertification control in Africa (Grant No. SAJC202108) and the key technical talent project of Chinese Academy of Sciences (Research on desertification technology along the “Belt and Road”) for financial support to do this paper. Our thanks also go to the support of the “Tianchi doctor program” of Xinjiang Uygur Autonomous Region in 2020.

Conflict of interests. The authors declare that they have no known competing financial or personal relationships that could have appeared to influence the work reported in this paper.

REFERENCES

[1] Aaviksoo, K. (1995): Simulating vegetation dynamics and land use in a mire landscape using a Markov model. – Landsc. Urban Plan. 31: 129-142. https://doi.org/https://doi.org/10.1016/0169-2046(94)01045-A.
[2] Abdullahi, M., Yakubu, A., Uba, G., Abdullahi, S. A. (2023): Enumeration of pathogenic bacteria from automatic teller machine (ATMs) keyboard, a case study of ATM machine

http://www.aloki.hu ● ISSN 1589 1623 (Print) ● ISSN 1785 0037 (Online)
DOI: http://dx.doi.org/10.15666/aeer/2204_36413676

of branch 448 Unity Bank Plc Jahun, Jahun Local Government, Jigawa State. – – Journal of Biochemistry, 11(2): 2-5.

[3] Abuzaid, A. S., Abdelatif, A. D. (2022): Assessment of desertification using modified MEDALUS model in the north Nile Delta, Egypt. – Geoderma 405(August 2021): 115400. https://doi.org/10.1016/j.geoderma.2021.115400.

[4] Afrin, S., Gupta, A., Farjad, B., Razu Ahmed, M., Achari, G., Hassan, Q. (2019): Development of land-use/land-cover maps using landsat-8 and MODIS data, and their integration for hydro-ecological applications. – Sensors (Switzerland): 19(22). https://doi.org/10.3390/s19224891.

[5] Ahmed, B., Ahmed, R. 2012. (2012): Modeling urban land cover growth dynamics using multioral satellite images: a case study of Dhaka, Bangladesh. – ISPRS. Int. J. Geo-Inf. 1. 3-31. https://doi.org/https://doi.org/10.3390/ijgi1010003.

[6] Araya, Y. H., Cabral, P. (2010): Analysis and modeling of urban land cover change in Setúbal and Sesimbra, Portugal. – Remote Sensing 2(6): 549-1563. https://doi.org/doi:10.3390/rs2061549.

[7] Audu, E. B. (2013): Fuelwood consumption and desertification in Nigeria. – International Journal of Science and Technology 3(1): 1-5. http://ejournalofsciences.org/archive/vol3no1_1.pdf.

[8] Baqa, M., Chen, F., Lu, L., Qureshi, S., Tariq, A., Wang, S., Jing, L., Hamza, S., Li, Q. (2022): Monitoring and modeling the patterns and trends of urban growth using urban sprawl matrix and CA-Markov model: a case study of Karachi, Pakistan from 2000 to 2020. – Remote Sensing 14(9): 2164.

[9] Benjaminsen, T. A., Hiernaux, P. 2019. (2019): From desiccation to global climate change: a history of the desertification narrative in the West African Sahel 1900-2018. – Global Environ. 12(1): 206-236. https://doi.org/https://doi.org/10.3197/ge.2019.120109.

[10] Bernabé, S., Plaza, A. (2010): A new system to perform unsupervised and supervised classification of satellite images from Google Maps. – Satellite Data Compression, Communications, and Processing VI 7810: 781010. https://doi.org/10.1117/12.863243.

[11] Berrahmouni, N., Laestadius, L., Martucci, A., Mollicone, D., Patriarca, C., Sacande, M. (2016): Building Africa's Great Green Wall: Restoring Degraded Drylands for Stronger and More Resilient Communities. – FAO, Rome.

[12] Brandt, M., Tucker, C. J., Kariryaa, A., Rasmussen, K., Abel, C., Small, J., Chave, J., Rasmussen, L. V., Hiernaux, P., Diouf, A. A., Kergoat, L., Mertz, O., Igel, C., Gieseke, F., Sch¨oning, J., Li, S., Melocik, K., Meyer, J., Sinno, S., Romero, E., Glennie, E., Montagu, A., Dendoncker, M., Fensholt, R. (2020): An unexpectedly large count of trees in the West African Sahara and Sahel. – Nature 587(7832): 78-82. https://doi.org/https://doi.org/10.1038/s41586-020-2824-5.

[13] Campbell, J. B. (2006): Introduction to Remote Sensing. – Guildford Press, New York.

[14] Chander, G., Coan, M. J., Scaramuzza, P. L. (2008): Evaluation and comparison of the IRS-P6 and the landsat sensors. – IEEE Transactions on Geoscience and Remote Sensing 46(1): 209-221. https://doi.org/10.1109/TGRS.2007.907426.

[15] Chen, L., Sun, Y., Saeed, S. (2018): Monitoring and predicting land use and land cover changes using remote sensing and GIS techniques—a case study of a hilly area, Jiangle, China. – PLoS ONE 13:(e0200493.).

[16] Congalton, R. G. (1991): A review of assessing the accuracy of classifications of remotely sensed data. – Remote Sensing of Environment 37: 35-46.

[17] Cotthem, W. (2007): About Drought, Desertification and Poverty in the Dry Lands. – https://desertification.wordpress.com/.

[18] D'Odorico, P., Bhattachan, A., Davis, K. F., Ravi, S., Runyan, C. W. (2013): Global desertification: drivers and feedbacks. – Advances in Water Resources 51: 326-344. https://doi.org/10.1016/j.advwatres.2012.01.013.

[19] da Silva, B. F., dos Santos Rodrigues, R. Z., Heiskanen, J., Abera, T. A., Gasparetto, S. C., Biase, A. G., Ballester, M. V. R., de Moura, Y. M., de Stefano Piedade, S. M., de

http://www.aloki.hu ● ISSN 1589 1623 (Print) ● ISSN 1785 0037 (Online)
DOI: http://dx.doi.org/10.15666/aeer/2204_36413676

Oliveira Silva, A. K., de Camargo, P. B. (2023): Evaluating the temporal patterns of land use and precipitation under desertification in the semi-arid region of Brazil. – Ecological Informatics 77(August 2022). https://doi.org/10.1016/j.ecoinf.2023.102192.

[20] Darkoh, M. B. K. (1989): Desertification in Africa. – Eastern African Research & Development 19: 1-50. https://doi.org/http://www.jstor.org/stable/24325608.

[21] Deng, J. S., Wang, K., Deng, Y. H., Qi, G. J. (2008): PCA-based land-use change detection and analysis using multitemporal and multisensor satellite data. – International Journal of Remote Sensing 29(16): 4823-4838. https://doi.org/10.1080/01431160801950162.

[22] Dimitrios Triantakonstantis, G. M. (2012): Urban growth prediction: a review of computational models and human perceptions. – Journal of Geographic Information System 4(6). https://doi.org/DOI:10.4236/jgis.2012.46060.

[23] do Nascimento, R. (2023): Causes and Impacts of Desertification in the World. – In: Global Environmental Changes, Desertification and Sustainability. Springer Nature, Cham. https://doi.org/10.1007/978-3-031-32947-0_4.

[24] Eduardo Garcia-Frapolli, Barbara Ayala-Orozco, M. B.-M., Celene Espadas-Manrique, G. R.-F. (2007): Biodiversity conservation, traditional agriculture and ecotourism: land cover/land use change projections for a natural protected area in the northeastern Yucatan Peninsula, Mexico. – Landscape and Urban Planning 87: 137-153. https://doi.org/doi:10.1016/j.landurbplan.2007.03.007.

[25] El-hallaq, M. A., Habboub, M. O. (2015): Using cellular automata-markov analysis and multi criteria evaluation for predicting the shape of the Dead Sea. – Advances in Remote Sensing 4(1): 83-95.

[26] Falaki, M. A., Ahmed, H. T., Akpu, B. (2020): Predictive modeling of desertification in Jibia Local Government Area of Katsina State, Nigeria. – Egyptian Journal of Remote Sensing and Space Science 23(3): 363-370. https://doi.org/10.1016/j.ejrs.2020.04.001.

[27] Fan, F., Wang, Y., Wang, Z. (2008): Temporal and spatial change detecting (1998-2003) and predicting of land use and land cover in Core corridor of Pearl River Delta (China) by using TM and ETM+ images. – Environ Monit Assess 137: 127-147. https://doi.org/https://doi.org/10.1007/s10661-007-9734-y.

[28] Food and Agriculture Organization (FAO) of the United Nations (2005): Nigeria: Global Forest Resources Assessment 2015 Country Report. – FAO, Rome. http://www.fao.org/3/a-au190e.pdf.

[29] Gharib, S. (2008): Synthesizing system dynamics and geographic information systems in a new method to model and simulate environmental systems. – Doctoral Thesis, University of Bergen.

[30] Ghayour, L., Neshat, A., Paryani, S., Shahabi, H., Shirzadi, A., Chen, W., Al-Ansari, N., Geertsema, M., Amiri, M. P., Gholamnia, M., Dou, J., Ahmad, A. (2021): Performance evaluation of sentinel-2 and landsat 8 OLI data for land cover/use classification using a comparison between machine learning algorithms. – Remote Sensing 13(7). https://doi.org/10.3390/rs13071349.

[31] Gomiero, T. (2016): Soil degradation, land scarcity and food security: reviewing a complex challenge. – Sustainability 8: 281.

[32] Hamdy, O., Zhao, S., Salheen, M. A., Eid, Y. Y. (2017): Analyses the driving forces for urban growth by using IDRISI ® Selva Models Abouelreesh Aswan as a case study. – Int. J. Eng. Technol. 9(3). https://doi.org/10.7763/IJET.2017.V9.975.

[33] Huang, G., Heokstra, A. Y., Krol, M. S., Galindo, A., Jägermeyr, J., Yu, C., Wang, R. (2020): Water-saving agriculture can deliver deep water cuts for China. – Resour. Conserv. Recycl. 154(104578). https://doi.org/doi={10.1016/j.resconrec.2019.104578}.

[34] Huang, J., Zhang, G., Zhang, Y., Guan, X., Wei, Y., Guo, R. (2020): Global desertification vulnerability to climate change and human activities. – Land Degradation and Development 31(11): 1380-1391. https://doi.org/10.1002/ldr.3556.

http://www.aloki.hu ● ISSN 1589 1623 (Print) ● ISSN 1785 0037 (Online)
DOI: http://dx.doi.org/10.15666/aeer/2204_36413676

[35] Huber-Sannwald, E., Martínez-Tagüena, N., Espejel, I., Lucatello, S., Coppock, D. L., Reyes Gomez, V. M. (2020): Introduction: international network for the sustainability of drylands-transdisciplinary and participatory research for dryland stewardship and sustainable development. – In: Lucatello, S. et al. (eds.) Stewardship of Future Drylands and Climate Change in the Global South: Challenges and Opportunities of the Agenda 2030. Springer, Cham. pp. 1-24. https://doi.org/10.1007/978-3-030-2246-6_1.

[36] Ibrahim, I. Y., Wang, Y. D., Zhou, N., Ibrahim, B. M., Umar, D. D., You, Y., ... Nasir, L. I. (2023): Assessment of remote sensing on deforestation of economic tree species in Wudil, Kano State, Nigeria. – Applied Ecology and Environmental Research 21(5): 4445-4474. https://doi.org/10.15666/aeer/2105_44454474.

[37] Jensen, J. R. (1996): Introductory Digital Image Processing: A Remote Sensing Perspective. 2nd Ed. – Prentice Hall, Inc., Upper Saddle River, NJ.

[38] Kassas, M. (1995): Desertification: a general review. – Journal of Arid Environments 30(2): 115-128.

[39] Koko, A. F., Han, Z., Wu, Y., Abubakar, G. A., Bello, M. (2022): Spatiotemporal land use/land cover mapping and prediction based on hybrid modeling approach: a case study of Kano Metropolis, Nigeria (2020-2050). – Remote Sensing 14(23). https://doi.org/10.3390/rs14236083.

[40] Lamchin, M., Lee, J. Y., Lee, W. K., Lee, E. J., Kim, M., Lim, C. H., Choi, H. A., Kim, S. R. (2016): Assessment of land cover change and desertification using remote sensing technology in a local region of Mongolia. – Advances in Space Research 57(1): 64-77. https://doi.org/10.1016/j.asr.2015.10.006.

[41] Li, X., Liu, L., Huang, L. (2020): Comparison of several remote sensing image classification. – – Int. Arch. Photogramm. Remote Sens. Spatial Inf. Sci., XLII-3/W10, 605-611. https://doi.org/10.5194/isprs-archives-XLII-3-W10-605-2020.

[42] Macarringue, L., Bolfe, É., Pereira, P. (2022): Developments in land use and land cover classification techniques in remote sensing: a review. – Journal of Geographic Information System 14: 1-8. https://doi.org/doi: 10.4236/jgis.2022.141001.

[43] Mansour, S., Alahmadi, M., Atkinson, P. M., Dewan, A. (2022): Forecasting of built-up land expansion in a desert urban environment. – Remote Sensing 14. https://doi.org/https://doi.org/10.3390/ rs14092037.

[44] Masson-Delmotte, V. (2019): Climate Change and Land: An IPCC Special Report on Climate Change, Desertification, Land Degradation, Sustainable Land Management, Food Security, and Greenhouse Gas Fluxes in Terrestrial Ecosystems: Summary for Policymakers. – Intergovernmental Panel on Climate Change, Geneva.

[45] Mohammed, F. Y., Ariori, N. A., Akoso, T. M., and Udofia, S. K. (2022): Assessment of the trend of desert encroachment dynamics in Northeastern Nigeria - a case study of Jigawa State. – AGU Fall Meeting Abstracts, NH45D-0481.

[46] Monirsadat, T., Mohamadhosein, A., Ghafary, G. (2011): Forecasting drought by Markov Chain in Ardakan city. – In: 21st International Conference on Irrigation and Drainage (ICID), pp. 213-218.

[47] Muhammad, I. (2020): Effects of flood on environmental quality in Ringim, Jigawa State, Northern Nigeria. – – International Journal of Science for Global Sustainability 6(3): 33-44.

[48] Mumtaz, F., Tao, Y., Leeuw, G. de, Zhao, L., Fan, C., Elnashar, A., Bashir, B., Wang, G., Li, L. L., Naeem, S., A. (2020): Modeling spatio-temporal land transformation and its associated impacts on land surface temperature (LST). – Remote Sensing 12. https://doi.org/https:// doi.org/10.3390/RS12182987.

[49] Muñoz-Marí, J., Bruzzone, L., Camps-Valls, G. (2007): A support vector domain description approach to supervised classification of remote sensing images. – IEEE Transactions on Geoscience and Remote Sensing 45(8): 2683-2692.

[50] Mushore, T. D., Mutanga, O., Odindi, J., Dube, T. (2016): Assessing the potential of integrated Landsat 8 thermal bands, with the traditional reflective bands and derived

http://www.aloki.hu ● ISSN 1589 1623 (Print) ● ISSN 1785 0037 (Online)
DOI: http://dx.doi.org/10.15666/aeer/2204_36413676

vegetation indices in classifying urban landscapes. – Geocarto International 1752-0762. https://doi.org/: 10.1080/10106049.2016.1188168.

[51] Olsson, L. (1993): Desertification in Africa - a critique and an alternative approach. – GeoJournal 31(1): 23-31. https://doi.org/10.1007/BF00815899.

[52] Pechanec, V., Purkyt, J., Benc, A., Nwaogu, C., Štěrbová, L., Cudlín, P. (2018): Modelling of the carbon sequestration and its prediction under climate change. – Ecological Informatics 47(August 2017): 50-54. https://doi.org/10.1016/j.ecoinf.2017.08.006.

[53] Policelli, F., Hubbard, A., Jung, H. C., Zaitchik, B., Ichoku, C. (2019): A predictive model for Lake Chad total surface water area using remotely sensed and modeled hydrological and meteorological parameters and multivariate regression analysis. – Journal of Hydrology 568: 1071-1080. https://doi.org/https://doi.org/10.1016/j.jhydrol.2018.11.037.

[54] Prasad, P., Loveson, V. J., Chandra, P., Kotha, M. (2022): Evaluation and comparison of the earth observing sensors in land cover/land use studies using machine learning algorithms. – Ecological Informatics 68(December 2021): 101522. https://doi.org/10.1016/j.ecoinf.2021.101522.

[55] Pravalie, R. (2021): Exploring the multiple land degradation pathways across the planet. – Earth Sci. Reviews 220: 10368(0012-8252). https://doi.org/https://doi.org/10.1016/j.earscirev.2021.103689.

[56] Pravalie, R., Patriche, C., Borrelli, P., Panagos, P., Roșca, B., Dumitrascu, M., Nita, I.-A., Savulescu, I., Birsan, M.-V., Bandoc, G. (2021): Arable land under the pressure of muliple land degredation processes. A global perspective. – Environmental Research 194(0013-9351). https://doi.org/https://doi.org/10.1016/j.envres.2020.110697.

[57] Rabiner, L. R. (1989): A tutorial on hidden Markov models and selected applications in speech recognition. – Proceedings of the IEEE 77(2): 257-286. https://doi.org/10.1109/5.18626.

[58] Reynolds, J. F., Stafford Smith, D. M., Lambin, E. F., Turner, B. L., Mortimore, M., Batterbury, S. P. J., Downing, T. E., Dowlatabadi, H., Fernández, R. J., Herrick, J. E., Huber-Sannwald, E., Jiang, H., Leemans, R., Lynam, T., Maestre, F. T., Ayarza, M., Walker, B. (2007): Global desertification: building a science for dryland development. – Science 316(5826): 847-851. https://doi.org/10.1126/science.1131634.

[59] Routh, D., Seegmiller, L., Bettigole, C., Kuhn, C., Oliver, C. D., Glick, H. B. (2018): Improving the reliability of mixture tuned matched filtering remote sensing classification results using supervised learning algorithms and cross-validation. – Remote Sensing 10(11). https://doi.org/10.3390/rs10111675.

[60] Rwanga, S. S., Ndambuki, J. M. (2017): Accuracy assessment of land use/land cover classification using remote sensing and GIS. – International Journal of Geosciences 08(04): 611-622. https://doi.org/10.4236/ijg.2017.84033.

[61] Schreiber, K. (2013): An Approach to Monitoring and Assessment of Desertification Using Integrated geospatial Technologies. – Millersville University, Pennsylvania.

[62] Shuai, J., Liu, J., Cheng, J., Cheng, X., Wang, J. (2021): Interaction between ecosystem services and rural poverty reduction: evidence from China. – Environmental Science & Policy 119: 1-11. https://doi.org/https://doi.org/10.1016/j.envsci.2021.01.011.

[63] Singh, S. K., Laari, P. B., Mustak, S., Srivastava, P. K., Szabo, S. (2018): Modelling of land use land cover change using earth observation data-sets of Tons River Basin, Madhya Pradesh, India. – Geocarto Int. 33: 1202-1222. https://doi.org/https://doi.org/10.1080/ 10106049.2017.1343390.

[64] Sop, T. K., Oldeland, J. (2013): Local perceptions of woody vegetation dynamics in the context of a 'Greening Sahel': a case study from Burkina Faso. – Land Degradation and Development 24(6): 511-527. https://doi.org/https://doi.org/10.1002/ldr.1144.

[65] Tariq, A., Shu, H. (2020): CA-Markov chain analysis of seasonal land surface temperature and land use land cover change using optical multi-temporal satellite data of

http://www.aloki.hu ● ISSN 1589 1623 (Print) ● ISSN 1785 0037 (Online)
DOI: http://dx.doi.org/10.15666/aeer/2204_36413676

Faisalabad, Pakistan. – Remote Sensing 12(20). https://doi.org/https://doi.org/10.3390/rs12203402.

[66] Tariq, A., Yan, J., Mumtaz, F. (2022): Land change modeler and CA-Markov chain analysis for land use land cover change using satellite data of Peshawar, Pakistan. – Physics and Chemistry of the Earth 128(October): 103286. https://doi.org/10.1016/j.pce.2022.103286.

[67] Tierney, J. E., Ummenhofer, C. C., deMenocal, P. B. (2015): Past and future rainfall in the Horn of Africa. – Science Advances 1(9). https://doi.org/https://doi.org/10.1126/sciadv.1500682.

[68] Tomasella, J., Silva Pinto Vieira, R. M., Barbosa, A. A., Rodriguez, D. A., de Oliveira Santana, M., Sestini, M. F. (2018): Desertification trends in the Northeast of Brazil over the period 2000-2016. – International Journal of Applied Earth Observation and Geoinformation 73(November 2017): 197-206. https://doi.org/10.1016/j.jag.2018.06.012.

[69] Tudunwada, I. Y. A. A. (2022): Flood vulnerability mapping and prediction for early warning in Jigawa State, Northern Nigeria, using geospatial techniques. – International Journal of Disaster Risk Reduction 79(2212-4209). https://doi.org/https://doi.org/10.1016/j.ijdrr.2022.103156.

[70] UN (2015): Transforming Our World: the 2030 Agenda for Sustainable Development. – https://sdgs.un.org/2030agenda.

[71] UNCCD (1992): United Nations Conference on Environment and Development, 3-14 June. – Rio de Janeiro, Brazil.

[72] Verma, P., Siddiqui, A. R., Mourya, N. K., Devi, A. R. (2024): Forest carbon sequestration mapping and economic quantification infusing MLPnn-Markov chain and InVEST carbon model in Askot Wildlife Sanctuary, Western Himalaya. – Ecological Informatics 79(December 2023): 102428. https://doi.org/10.1016/j.ecoinf.2023.102428.

[73] Wang, C., Komodakis, N., Paragios, N. (2013): Markov random field modeling, inference & learning in computer vision & image understanding: a survey. – Comput. Vis. Image Understand 117: 1610-1627. https://doi.org/https://doi.org/10.1016/j.cviu.2013.07.004.

[74] Wang, T. (2003): Sandy desertification in North China. – Sci. China Ser. D-Earth Sci. 45(December): 359-371. https://doi.org/10.1142/9789812705150_0041.

[75] White, R., Engelen, G., Uljee, I. (2001): Modeling land use change with linked cellular automata and socio-economic models: a tool for exploring the impact of climate change on the Island of St. Lucia. – https://api.semanticscholar.org/CorpusID: 17820

[76] Williams, a. P., Seager, R., Abatzoglou, J., Cook, B., Smerdon, J., Cook, E. (2015): to California drought during 2012-2014. – Geophysical Research Letters 1-10. https://doi.org/10.1002/2015GL064924.Received.

[77] Yang, Z., Gao, X., Lei, J., Meng, X., Zhou, N. (2022): Analysis of spatiotemporal changes and driving factors of desertification in the Africa Sahel. – Catena 213(February): 106213. https://doi.org/10.1016/j.catena.2022.106213.

[78] Yunusa, M. (2012): Desertification livelihood, challenges and urban development: an observation. – National Conference of the Nigerian Institute of Town Planners 89-96.

[79] Zangina, A. S., Sa'adu, S. D., Abubakar, A. (2019): Transition from land use/cover into urban expansion in Dutse Metropolis, Jigawa State, Nigeria. – Themes in Applied Sciences Research 2(1): 1-8. https://doi.org/10.33094/journal.140.2019.21.1.8.

[80] Zeng, Y., Xiang, N., Feng, Z., Xu, H. (2006): Albedo-NDVI space and remote sensing synthesis index models for desertification monitoring. – Scientia Geographica Sinica 26(1): 75-81. https://doi.org/https://doi.org/10.3969/j.issn.1000-0690.2006.01.013.

[81] Zongfan, B., Ling, H., Xuhai, J., Ming, L., Liangzhi, L., Huiqun, L., Jiaxin, L. (2022): Spatiotemporal evolution of desertification based on integrated remote sensing indices in Duolun County, Inner Mongolia. – Ecological Informatics 70(May): 101750. https://doi.org/10.1016/j.ecoinf.2022.101750.

http://www.aloki.hu ● ISSN 1589 1623 (Print) ● ISSN 1785 0037 (Online)
DOI: http://dx.doi.org/10.15666/aeer/2204_36413676

APPENDIX

Figure A1. *(a) Visualization of desertification approach in the study area. (b) Approach to Desertification in the Study Area's Metropolis. (c) Approach to desertification in farmlands in the research region. (Source: Authors' analysis)*

http://www.aloki.hu ● ISSN 1589 1623 (Print) ● ISSN 1785 0037 (Online)
DOI: http://dx.doi.org/10.15666/aeer/2204_36413676